

**IDENTIFICATION AND DIFFERENTIATION OF  
INDIVIDUAL BETA EMITTERS IN WASTE MIXTURES  
BY LIQUID SCINTILLATION SPECTROMETRY**

A Thesis

by

ROBIN LYNN SISKEL

Submitted to the Graduate College of  
Texas A&M University  
in partial fulfillment of the requirements for the degree of

MASTER OF SCIENCE

May 1988

Major Subject: Health Physics

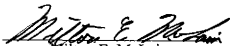
IDENTIFICATION AND DIFFERENTIATION OF  
INDIVIDUAL BETA EMITTERS IN WASTE MIXTURES  
BY LIQUID SCINTILLATION SPECTROMETRY

A Thesis

by

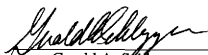
ROBIN LYNN SISSEL


Approved as to style and content by:

  
Milton E. McLain  
(Chairman)

  
John W. Poston, Sr.  
(Member)

  
Dan Hightower  
(Member)

  
Gerald A. Schlapper  
(Member)

  
Kenneth L. Peddicord  
(Head of Department)

May 1988

## ABSTRACT

### **Identification and Differentiation of Individual Beta Emitters in Waste Mixtures by Liquid Scintillation Spectrometry. (May 1988)**

Robin Lynn Siskel, B.S., Texas A&M University

Chairman of Advisory Committee: Dr. Milton E. McLain

Recent regulatory changes allow non-radioactive disposal of low activity carbon-14, tritium, and iodine-125 liquid scintillation wastes, provided that the activity and isotopes present can be documented. This legislation has generated a significant interest in developing a quick, cost efficient method of identification and differentiation of various beta emitting isotopes within waste mixtures.

A state-of-the-art liquid scintillation spectrometer and incorporated multichannel analyzer was used to identify and evaluate techniques suitable for unknown liquid sample identification. Differentiation of various components within a two isotope mixture, and the detection level of a small activity of one nuclide in a large activity of a second radioisotope was examined. A catalogue of spectra, including the isotopic ratio of each component in the mixture, and pure spectra was compiled for use as reference data. This catalogue included both pure spectrum, and various mixtures of tritium, carbon-14, iodine-125, calcium-45, sulfur-35, and phosphorus-32.

A technique including visual comparison to reference data was the most practical method of unknown identification, and fully complies with regulatory requirements for relatively unquenched sample mixtures of two isotopes. Accurate isotopic identification and differentiation was found to be feasible up to a 1 : 50 ratio for most of the research radio-nuclides. Approximate minimum detectable activities of 0.17 to 0.45 pCi, and lower limits of detection from 1.00 to 0.37 pCi were calculated for the isotopes used in this research.

## ACKNOWLEDGMENT

There are many people throughout both my past and present that I would very much like to thank for their friendship, guidance, and advice -- for without them this work would most likely not have turned out as it is. I would like to thank the Texas A&M Nuclear Engineering department and Dr. Erdman for the opportunity to pursue this degree, and for financial support.

I am especially grateful to my committee members, and would like to offer them the warmest of thanks: Dr. McLain for his endless patience and timely reviews of this manuscript, Dr. Poston for his constant help and understanding (offered at any hour), Dr. Schlapper for every word of encouragement and expert guidance, and Dr. Hightower for his advice.

I would furthermore like to give special thanks to my Dad for his wonderful encouragement and sound, logical advice throughout the good times and bad, and to my Mom and my brother for all of their support and love. As we all wind our way through the many varied paths of life, I feel that I have been incredibly lucky to have been able to share mine with some of the most wonderful people in the world.

## TABLE OF CONTENTS

	Page
ABSTRACT .....	iii
ACKNOWLEDGMENT .....	iv
TABLE OF CONTENTS .....	v
LIST OF FIGURES .....	vi
LIST OF TABLES .....	ix
INTRODUCTION .....	1
THEORY .....	6
History of the Liquid Scintillation Method .....	6
Basic Principles .....	7
Hardware and Accessories .....	18
EQUIPMENT AND PROCEDURES .....	29
The Liquid Scintillation Spectrometer .....	29
Experimental Procedures .....	33
RESULTS .....	37
General Information .....	37
Sample Spectra .....	37
CONCLUSIONS .....	79
Calculation of LLD and MDA .....	79
Sample Spectra .....	79
RECOMMENDATIONS FOR FUTURE RESEARCH .....	83
REFERENCES .....	85
APPENDIX A SPECTROMETER OPERATIONAL FLOW CHART .....	87
APPENDIX B PROGRAMS AND COMMAND FILES .....	88
APPENDIX C CALCULATION OF LLD's AND MDA's .....	92
VITA .....	96

## LIST OF FIGURES

FIGURE	Page
1 Interaction of beta particle with cocktail .....	8
2 Spectral response of typical bi-alkali photocathode .....	11
3 Chemical composition of a common fluor .....	12
4 Absorption and emission spectrum of PPO .....	13
5 Effect of quenching on a LSD pulse-height spectrum .....	15
6 Concentration dependency on scintillation yield .....	16
7 Basic components of a liquid scintillation counter .....	20
8 Basic construction of a linear type photomultiplier tube .....	22
9 Schematic of a LSC with attached MCA .....	25
10 Basic principles of an analog-to-digital converter .....	27
11 Layout of the LKB-Wallac 1219 Rackbeta 'Spectral' Liquid Scintillation Spectrometer .....	30
12 Spectra of pure radioisotopes: Left axis; C-14, I-125, H-3. Right axis; P-32, S-35, Ca-45 .....	39
13 Spectra of pure radioisotopes on a logarithmic scale: Left axis; Ca-45, H-3, C-14. Right axis; I-125, S-35, P-32 .....	40
14 Comparison of typical background spectra on linear versus logarithmic scales .....	41
15 Iodine-125 in varying amounts of carbon-14; ratios from 1 : 7.1 to 1 : 5.5 .....	44
16 Iodine-125 in varying amounts of carbon-14; ratios from 1 : 7.1 to 1 : 12.9 .....	45
17 Iodine-125 in varying amounts of carbon-14; ratios from 1 : 14.6 to 1 : 26.9 .....	46
18 Iodine-125 in varying amounts of carbon-14; ratios from 1 : 30.2 to 1 : 48.9 .....	47

19	Comparison of 1 iodine-125 to 48.9 carbon-14 on linear versus logarithmic scales .....	48
20	Calcium-45 in varying amounts of carbon-14; ratios from pure calcium-45 to 1 : 6.1 .....	49
21	Calcium-45 in varying amounts of carbon-14; ratios from 1 : 10.5 to 1 : 51.1 .....	50
22	Comparison of 1 calcium-45 to 51.1 carbon-14 on linear versus logarithmic scales .....	51
23	Phosphorus-32 in varying amounts of carbon-14; ratios from pure P-32 to 1 : 6.5 .....	52
24	Phosphorus-32 in varying amounts of carbon-14; ratios from 1 : 14.9 to 1 : 45.2.....	53
25	Comparison of 1 phosphorus-32 to 45.2 calcium-14 on linear versus logarithmic scales .....	54
26	Sulfur-35 in varying amounts of carbon-14; ratios from pure S-35 to 1: 5.6 .....	55
27	Sulfur-35 in varying amounts of carbon-14; ratios from 1 : 10.2 to 1 : 51.0 .....	56
28	Comparison of 1 sulfur-35 to 51.0 carbon-14 on linear versus logarithmic scales.....	57
29	Iodine-125 in varying amounts of tritium; ratios from pure I-125 to 1 : 4.9 .....	58
30	Iodine-125 in varying amounts of tritium; ratios from 1 : 9.4 to 1 : 30. ....	59
31	Comparison of 1 iodine-125 to 30.0 tritium on linear versus logarithmic scales .....	60
32	Calcium-45 in varying amounts of tritium; ratios from pure Ca-45 to 1 : 7.7 .....	61
33	Calcium-45 in varying amounts of tritium; ratios from 1 : 15.2 to 1 : 36.2 .....	62
34	Comparison of 1 calcium-45 to 36.2 tritium on linear versus logarithmic scales .....	63

35	Phosphorus-32 in varying amounts of tritium; ratios from pure P-32 to 1 : 5.1 .....	64
36	Phosphorus-32 in varying amounts of tritium; ratios from 1 : 12.5 to 1 : 31.2 .....	65
37	Comparison of 1 phosphorus-32 to 31.2 tritium on linear versus logarithmic scales .....	66
38	Sulfur-35 in varying amounts of tritium; ratios from pure S-35 to 1 : 4.8 .....	67
39	Sulfur-35 in varying amounts of tritium; ratios from 1 : 4.8 to 1 : 33.1 .....	68
40	Comparison of 1 sulfur-35 to 33.1 tritium on linear versus logarithmic scales .....	69
41	Calcium-45 in varying amounts of iodine-125; ratios from pure Ca-45 to 1 : 5.8 .....	70
42	Calcium-45 in varying amounts of iodine-125; ratios from 1 : 10.5 to 1 : 47.3 .....	71
43	Comparison of 1 calcium-45 to 47.3 iodine-125 on linear versus logarithmic scales .....	72
44	Phosphorus-32 in varying amounts of iodine-125; ratios from pure P-32 to 1 : 7.0 .....	73
45	Phosphorus-32 in varying amounts of iodine-125; ratios from 1 : 8.7 to 1 : 47.4 .....	74
46	Comparison of 1 phosphorus-32 to 47.4 iodine-125 on linear versus logarithmic scales .....	75
47	Sulfur-35 in varying amounts of iodine-125; ratios from pure sulfur-35 to 1 : 5.4 .....	76
48	Sulfur-35 in varying amounts of iodine-125; ratios from 1 : 10.2 to 1 : 46.4.....	77
49	Comparison of 1 sulfur-35 to 46.4 iodine-125 on linear versus logarithmic scales .....	78



**LIST OF TABLES**

<b>TABLE</b>		<b>Page</b>
1	Current yearly radioactive waste disposal costs .....	2
2	Proposed yearly non-radioactive waste disposal costs .....	2
3	Research radioisotopes and relevant values .....	4
4	Sample radioisotope acquisition, activity, and volume data .....	35
5	Calculated LLD and MDA Values .....	80
6	Maximum Determination Levels For Isotopic Combinations .....	81

## INTRODUCTION

Recent regulatory changes by the United States Nuclear Regulatory Commission and Agreement States allow disposal of carbon-14, iodine-125, and tritium in liquid scintillation cocktail wastes without regard to their radioactivity provided that the activity of each is less than 0.05  $\mu\text{Ci/mL}$  (NRC85). The Texas Department of Health, Bureau of Radiation Control, in the Texas Regulations for Control of Radiation part 21, section 307 (Disposal of Specific Waste), states specifically that (TDH86):

- (a) Any licensee may dispose of the following licensed material without regard to its radioactivity:
  - (1) 0.05 microcuries or less of hydrogen-3, carbon-14, or iodine-125, per gram of medium, used for liquid scintillation counting or *in vitro* clinical or *in vitro* laboratory testing...

And that:

- (b) Each licensee who disposes of material described in 21.307 (a) shall:
  - (1) make surveys adequate to assure that the limits of 21.307 (a) are not exceeded...

Numerous Texas A&M University (TAMU) facilities such as the Nuclear Science Center, Radiological Safety Office (RSO), and various campus research laboratories generate a significant amount of radioactive wastes whose disposal is allowed under these

-----

This thesis follows the style of Health Physics

regulations. The cost effectiveness for disposal of these radioisotope wastes would be greatly enhanced if it were possible to easily comply with the above stated regulations. The approximate costs of disposal as radioactive wastes is shown in Table 1.

TABLE 1. CURRENT YEARLY RADIOACTIVE WASTE DISPOSAL COSTS.

---

Price of drums: 300 drums/year @ \$30.00/drum = \$ 9,000
Price of disposal: 300 drums/year @ \$185.00/drum = \$ 55,500
Price of shipping: 300 drums/year @ \$30.00/drum = \$ 3,000
<b>Total Yearly Costs = \$67,500</b>

---

Compliance with the new regulations would allow such wastes to be discarded as non-radioactive for approximately the cost shown in Table 2.

TABLE 2. PROPOSED YEARLY NON-RADIOACTIVE WASTE DISPOSAL COSTS.

---

Price of drums: 300 drums/year @ \$2.00/drum = \$600.00
Price of disposal: 300 drums/year @ \$3.00/drum = \$900.00
Price of shipping: 300 drums/year @ \$2.00/drum = \$600.00
Price of additional employee = \$6,000.00
<b>Total Yearly Costs = \$8,100.00</b>

---

To take advantage of the regulation, liquid scintillation cocktail containing only tritium, iodine-125, and carbon-14 must be segregated from mixtures that include other radionuclides, and accurately assayed as to activity and concentration. It is, therefore, incumbent on the licensee to demonstrate and document that:

- (1) The concentrations of the three acceptable radionuclides are at or below the

specified limit, and;

- (2) Other radioactive materials are not present.

Until recently, such tasks and documentation were very difficult to accomplish cheaply and easily. Reliance on procedural controls may prove inadequate. Simply having researchers segregate nuclides by type is unreliable, since accidental mixing of waste containers is always possible.

The liquid scintillation method has been reliably used since the 1950's for beta detection in appropriate scintillation cocktails (No79). Carbon-14 and tritium are both relatively low energy pure beta emitters. The liquid scintillation counter (LSC) is commonly the method of choice for measuring these radionuclides. Single channel analyzers (SCAs) traditionally incorporated into the LSC system allow the selection of a range of pulse heights so data pertaining to the specific nuclide of interest can be accumulated even when counting a sample containing a mixture of radioactive species. Single channel analyzers, however, cannot easily cover the lower energy ranges in detail, nor do they readily allow thorough inspection of spectral detail in compound mixtures (Ed79) when compared to use of a multi-channel analyzer system. Thus, some method for easily and reliably identifying and quantifying the amount of each nuclide in a mixture of isotopes is needed.

Recently an LKB-Wallac 1219 RackBeta 'Spectral'\* liquid scintillation spectrometer (henceforth referred to as the Spectral) was purchased by the Texas A&M Department of Nuclear Engineering. This state of the art system has some unique features. The Spectral is intended to automatically count up to 300 samples of beta emitting radionuclides with energies in the range of 1 to 2000 keV (LKB87a). The incorporated multichannel analyzer and computer interface readily allows a much more accurate determination of the types and

\*LKB-Diagnostics, Co., Gaithersburg, Maryland.

quantities of radionuclides in a mixed sample than has been previously possible. With this system, a complete beta spectrum is collected, displayed, and stored on computer disk for further calculations.

Studies have not been conducted to determine whether mixtures of radioisotopes can be accurately identified and quantified using such a system prior to this research. Utilization of the Spectral to analyze and quantify TAMU waste mixtures so that solutions containing only carbon-14, tritium, and iodine-125 can be disposed of as non-radioactive wastes was proposed. The common radionuclides used in TAMU facilities and likely to be present in waste mixtures are phosphorus-32, calcium-45, sulfur-35, carbon-14, tritium, and iodine-125. These six nuclides were included in this study. Table 3 lists the decay modes and energies for each of these nuclides (Ge77).

TABLE 3. RESEARCH RADIOISOTOPES AND RELEVANT VALUES.

ISOTOPE	PRIMARY DECAY MODE	MAXIMUM ENERGY (MeV)	HALF-LIFE
H-3	$\beta^-$	0.0186	12.33 YEARS
Ca-45	$\beta^-$ $\gamma$	0.257 0.0124	163 DAYS
C-14	$\beta^-$	0.156	5730 YEARS
I-125	$\gamma$ E*	0.0355 0.177	59.7 DAYS
P-32	$\beta^-$	1.710	14.28 DAYS
S-35	$\beta^-$	0.1675	87.2 DAYS

\*Conversion Electron, and associated energy.

The objective of this research was to compile information on the spectra of beta emitting radionuclides as measured on the Spectral liquid scintillation spectrometer. This "pure" research information on radioactive mixtures of beta emitters can then be applied to practical waste disposal management. A reference spectra catalogue for the nuclides of interest was compiled. Use of the Spectral to identify individual nuclides and differentiate between multiple isotopes in a mixture was investigated. Means for spectra curve stripping was studied. A set of spectra for increasing ratios of calcium-45, sulfur-35, and phosphorus-32 individually mixed with first tritium, then carbon-14, and finally iodine-125 was constructed. Unknown isotope samples can then be identified by comparison to the generated reference curves. "Minimum detectable activities" (MDA) for each secondary radionuclide were determined for waste liquids containing tritium, carbon-14, and iodine-125. Finally, an algorithm for a computer program to automatically identify components in an unknown sample was proposed. In a university setting, it is unlikely that mixtures of more than two isotopes will be found. For this reason tritium, carbon-14, and iodine-125 were considered the nuclide of interest, and calcium-45, sulfur-35, and phosphorus-32 as contaminants. The scope of this study, therefore, was limited to binary radioisotope mixtures (i.e., two isotopes per sample), from a minimum of a 1 : 1 ratio, up to a maximum ratio of 1 : 50 for each nuclide combination.

This research demonstrates an expansion of the practical uses of liquid scintillation detectors with an incorporated multichannel analyzer. Furthermore, this investigation helped determine the degree to which the TAMU Radiological Safety Office, and similar facilities elsewhere, can take advantage of the recent regulatory changes regarding disposal of low-level liquid wastes.

## THEORY

### HISTORY OF THE LIQUID SCINTILLATION METHOD

Once it was realized that the passage of a charged particle through certain types of matter (called phosphors) caused a subsequent release of fluorescent energy, the study of scintillation detection had begun. After its initial development, the scintillation method of radiation detection was relatively ignored for a period of approximately fifteen years. The renaissance of the scintillation method began with the development of the photomultiplier (PM) tube in the 1930's. In 1947 H. Kallmann published a well read article which launched the study and use of organic scintillators (Ka47). In 1953, only six years later, J. B. Birks (one of the most well known pioneers in the field of scintillator studies) published the first book which covered many of the principles and uses of scintillation detectors. Even at that early date the value of the liquid scintillation method was realized. In his preface Birks stated that (Bi53; p. vii):

The scintillation counter is an instrument of great versatility and interest. In its original visual form it played a major role in the development of *classical* nuclear physics, from the identification of the  $\alpha$ -particle and the discovery of the atomic nucleus up to the Cockcroft-Walton experiments which initiated the "machine-age" of modern physics.

In its initial form, fluorescence from the scintillation counter was observed by the oldest known detector -- the human eye. The development of the PM tube, which converts the light photons into electronic pulses, allowed much more reliable and feasible instruments and methods to be instituted and applied.

Development of the liquid scintillation detector has relied on, and contributed to the technology of almost all fields of science, including physics, biology, biochemistry, chemistry, and many more. In the early 1950's, Ott reported that (Ot80):

Utilization of coincidence and fast discriminator circuitry, refrigeration of the phototubes, and use of PPO as solute were made in the first practical counter at

Los Alamos. Many applications of the system (and improved versions) were soon made, including counting of tritium-labeled water and organic compounds...

The rapid development of scintillators and equipment made reliable assays of low-energy beta emitters possible -- previously a very difficult task. Prior to liquid scintillation counting (LSC), gas counting was the only feasible method for tritium determinations, and carbon-14 had to be counted as a solid ( $\text{BaCO}_3$ ) or a gas ( $\text{CO}_2$ ). Both of these methods had many associated problems, whereas the detection of low-energy beta emitters proved to be the *forte* of LSC. LSC counting efficiencies for tritium have been increased greatly over the years -- from 10% in 1954 to greater than 60% today. Over the same time period, efficiencies for carbon have gone from 75% to almost 100%. Advances in PM tube design (e.g., the "bi-alkali" tube which has low thermionic noise at room temperature) have been in large part responsible for the increase in counting efficiencies.

## BASIC PRINCIPLES

Put in the simplest terms, the liquid scintillation method is a sequence of events in which emitted  $\beta$  particles collide with solvent molecules thus causing ionization and/or excitation of the atoms and molecules involved. When the ionized or excited products return to a ground state of energy (or recombine) energy is released. This energy interacts with one or two solutes (often referred to as primary and secondary fluors, respectively) which, in turn, emit detectable light in proportion to the initial  $\beta$  energy. Collision with solvent molecules and concomitant energy loss is repeated until all kinetic energy has been lost to the solvent and the  $\beta$  particle is captured. This process is depicted in Figure 1. It should be understood that only approximately 5% of the  $\beta$  particle total energy is finally observed as light (Co77; p. 70). The remainder of the energy is converted primarily to heat and lost to the scintillation process.



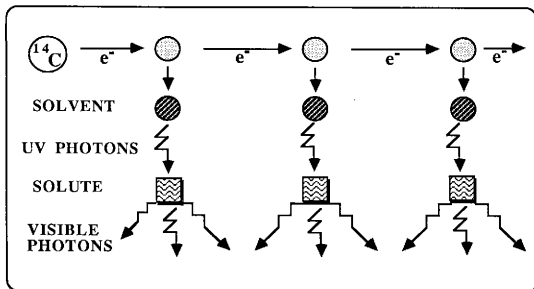


FIGURE 1: INTERACTION OF BETA PARTICLE WITH COCKTAIL.

- denotes solvent molecule in ground state;
- ◐ denotes solvent molecule in triplet state.

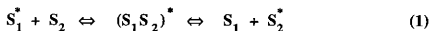
#### Energy Transfer

The initial energy transfer from the  $\beta$  particle to solvent occurs most efficiently in organic aromatic solvents, which are primarily low-density, low-Z materials. For this reason LSC is inefficient for the detection of penetrating radiation such as medium- and high-energy x or  $\gamma$ -rays. The intimate contact between the radioactive sample and scintillant, however, makes LSC the method of choice for detection of low energy x- or  $\gamma$ -rays, and  $\beta$  particles. These types of radiation cannot be counted efficiently by NaI (Tl) solid scintillation or semiconductor detectors because of absorption in the thickness of can material required around the detector (So80; p.246) and self-absorption within the sample (Ce83).

For LSC to be efficient, adequate energy transfer from sample to solvent and from solvent to solute must occur. The solvent must be able to dissolve not only the radioactive sample, but also the scintillator solute to ensure efficient energy exchange. The appropriate

mixture of solvent, solute, and any additives necessary to ensure dissolution or suspension of samples is referred to as the liquid scintillation "cocktail".

Luminescence is a general term used to describe the emission of light from a molecule in the excited state. This terminology is further refined to describe emission from the singlet excited state as fluorescence, and from the triplet excited state as phosphorescence. A measure of the time required for  $1/e$  of the excited molecules to emit photons is called the *lifetime*. Fluorescence decay lifetimes are on the order of  $10^{-5}$  to  $10^{-9}$  seconds, whereas phosphorescence has a much longer lifetime. Although the energy embodied in an excited solvent molecule may be emitted as a phosphorescent event, the measured lifetime of organic scintillators corresponds to that of a fluorescent event. The primary energy transfer in liquid scintillation mixtures occurs between solvent molecules. Two theories regarding the actual energy transfer mechanism between solvent molecules have been proposed. Birks suggested that solvent "eximers" (dimers of an excited molecule joined to an unexcited molecule -- Equation 1) are formed which eventually dissociate transferring excitation to the previously unexcited molecule (Bi53; p. 66).



Where  $S_1$  and  $S_2$  are solvent molecules and \* indicates the excited state. Voltz and co-workers theorized direct transfer via energy migration from one solvent molecule to its adjacent neighbors as shown in Equation 2 *without* the formation of an intermediate excited state molecule that Birks had postulated (Vo63).



Both of these methods are equilibrium processes, thus not every contact yields energy

transfer. Horrocks reports that the transfer process between solvent molecules occurs in a sub-nanosecond time frame and can occur over a distance of several molecular diameters (Ho74; p. 20). Furthermore, addition of a "diluter" (molecules which do not participate in the energy transfer process) decreases the efficiency of solvent-solvent energy transfer, implying that the transfer of energy is, in part, diffusion controlled. Light photon energy emitted by the solvent is typically on the order of 260 to 340 nm -- wavelengths too short (ultraviolet) to be readily detected by available photomultiplier tubes. The spectral response of a typical photocathode (and therefore photomultiplier tube) is shown in Figure 2.

To produce light of a detectable wavelength, a solute that is capable of fluorescing in the visible region is added. The solute (often referred to as the primary fluor) gains energy from the solvent through a resonance process that occurs in approximately  $10^{-11}$  seconds. Unlike the solvent-solvent energy transfer, the solvent-solute energy exchange is not diffusion controlled. The rate of energy exchange  $k$  when the solvent (donor) and solute (acceptor) are separated by the distance  $R$  can be calculated using Equation 3.

$$k = \frac{1}{\tau_0} \left( \frac{R_0}{R} \right)^6 \quad (3)$$

In this equation,  $\tau_0$  is the radiative decay time of the donor molecule, and  $R_0$  -- the critical transfer distance as defined by Forster (Fo59) -- is calculated by Equation 4.

$$R_0^6 = \frac{(9000 \ln 10) K^2}{128 \pi^5 n^4 N} \int_0^{\infty} F_D(\bar{\nu}) \epsilon_A(\bar{\nu}) \frac{d\bar{\nu}}{\bar{\nu}^4} \quad (4)$$

$K$  is an orientation factor,  $n$  the refractive index of the solvent,  $N$  Avogadro's number,  $F_D(\bar{\nu})$  the spectral distribution of the fluorescence emission of the donor molecule, and  $\epsilon_A$

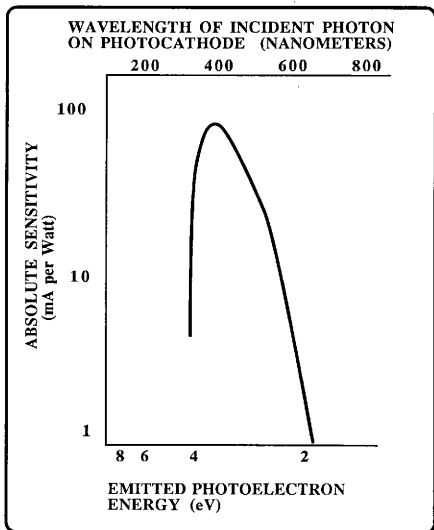


FIGURE 2. SPECTRAL RESPONSE OF TYPICAL BI-ALKALI PHOTOCATHODE.

(v) the molar decadic extinction coefficient of the acceptor molecule (Ho74; p. 22). It can be seen that energy transfer is dependent on specific qualities of the donor molecule, the distance separating donor and acceptor, and the qualities of the acceptor molecule. Thus, it is intuitively obvious that different combinations of solvents and solutes will have widely different energy transfer characteristics. The light output of such combinations can be compared to that of other cocktails to obtain a value for the relative scintillation efficiency of various solvents, solutes, or cocktail mixtures.

One of the most commonly used solutes, 2,5-diphenyloxazole (PPO), absorbs wavelengths from less than 260 nm to approximately 340 nm. Greatest PPO absorption, however, occurs between 290 nm and 320 nm -- ideal for energy transfer from typical solvents such as toluene or xylene. Figure 3 details the chemical composition of PPO.

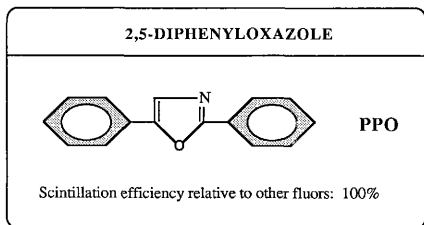


FIGURE 3: CHEMICAL COMPOSITION OF A COMMON FLUOR.

The absorption spectrum of PPO is shown in Figure 4. Some older LSC instruments were constructed with PM tubes that have a very limited sensitivity in the near UV range and therefore require light of an even longer wavelength than that emitted by PPO. In such cases, a secondary fluor (or 'wavelength shifter') is added which emits fluorescent light with a maximum intensity in the visible range of 420 nm to 440 nm (Co77; p. 73). POPOP (1,4-di-[2-5-phenyloxazole]-benzene) is one of the more common secondary fluors. Because the solute concentration is quite small relative to the solvent, the distance between solute molecules is generally significantly greater than the critical transfer distance  $R_c$ . Exceeding the critical transfer distance implies that the probability of solute-solute energy exchange is small, and conversely that the probability of fluorescence is large. The vibrational relaxation of the 'wavelength shifter' traps the energy of the primary solute, and thus sets the stage for fluorescent release from the secondary solute. Energy transfer between

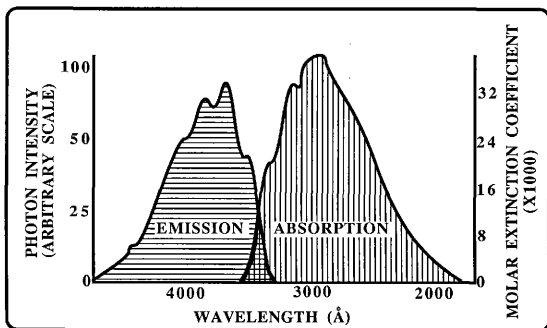


FIGURE 4: ABSORPTION AND EMISSION SPECTRUM OF PPO.

primary solutes, or between secondary solutes is relatively negligible. The photon energy  $E$  (in joules) released by a solute molecule is equal to the product of the photon frequency  $f$  (in hertz) and times Planck's constant  $h$  (Equation 5).

$$E = hf \quad (5)$$

When considered as a wave, the photon's frequency may be found using classical wave mechanics (Equation 6) where the velocity  $v$  (meters/sec) with which a wave travels is equal to the product of the wavelength  $\lambda$  (meters) and the frequency  $f$  ( $\text{sec}^{-1}$ ) of the wave.

$$f = \frac{v}{\lambda} \quad (6)$$

It should always be remembered that the total number of photons ultimately produced is proportional to the number of excited molecules originally present. While it is not within the scope of this document to go into a thorough discussion of the wave mechanics related to excitation states within molecules (any college level physical chemistry text may be consulted for a more thorough understanding of the principles involved), it should be noted that different excitational states and kinetic energies are possible in the scintillation process. Thus, a range of light wavelengths is produced. The total light output will be proportional, however, to the energy deposited in the LSC solvent by the energetic  $\beta$  particle. This energy deposition results in a relatively elongated light pulse produced in the scintillation cocktail over a short time span, rather than an instantaneous flash.

A thorough understanding of the advantages, disadvantages, and reasonable combinations of various solvents, fluors, and additives may be found in "Applications of Liquid Scintillation Counting", chapter III, by Donald L. Horrocks (Ho74).

### Quenching

Interference with any stage of the energy transfer or scintillation induced fluorescence processes is referred to as quenching. Quenching causes an apparent shift of the energy spectra to lower energy channels. Should the quenching shift part of the spectrum below the detector limits, a loss of counts will result. Quenched and unquenched sample spectra are shown in Figure 5. Three basic types of quenching must be considered:

- (1) Concentration quenching
- (2) Chemical quenching
- (3) Color quenching

As previously discussed, the efficiency of transfer of energy from the solvent to solute is dependent on the solute concentration. Should the concentration of solute be too small or large, the energy transfer process is hindered, and the counting efficiency is decreased.

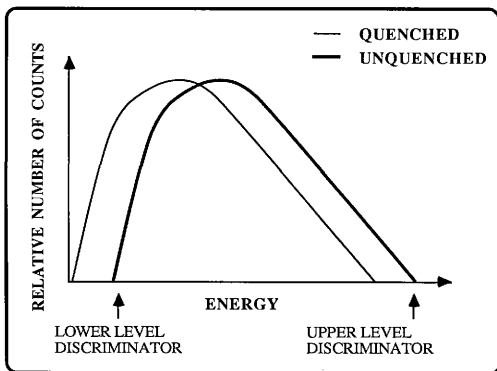


FIGURE 5: EFFECT OF QUENCHING ON A LSD PULSE-HEIGHT SPECTRUM.

This process is referred to as concentration quenching. Concentration quenching may also be caused by the addition of too large a sample relative to the amount of cocktail present (this is often referred to as "dilution" quenching). Concentration quenching may be diminished by adjusting the solute concentration such that the minimum amount of solute that provides a maximum of energy transfer is present once a sample is added to the cocktail. Figure 6 (Ho74; p. 47) depicts the concentration dependency of several common fluors on the scintillation yield as determined by the relative pulse height of the Compton edge produced by 662-keV gamma rays in toluene. Concentration quenching has relatively little effect on the counting efficiency for higher-energy  $\beta$  emitters, but a large effect on low-energy emitters such as  $^3\text{H}$ .

Chemical quenching occurs when substances compete with the primary fluor for absorption of energy but are not themselves scintillators, or when a substance modifies the



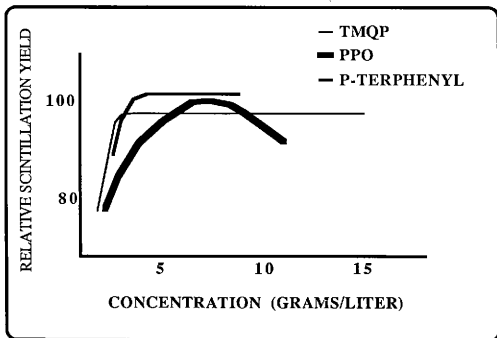


FIGURE 6: CONCENTRATION DEPENDENCY ON SCINTILLATION YIELD.

scintillate (solvent or solute molecules) to a nonfluorescing state. Chemical quenching can be caused by a wide variety of substances, most notably dissolved oxygen, strong acids, and strong bases. Avoiding the addition of any substances which could cause chemical quenching, or removing such substances from samples before adding cocktail will minimize chemical quenching.

Color quenching, on the other hand, does not affect the production of photons, but instead absorbs light produced by the solute. Water, blood, and colored substances produce color quenching. Dirty scintillation vials also produce a type of color quenching. It is obvious that any material which absorbs light in the 200 to 440 nm range would be expected to quench (Co77; p. 88). Avoiding the use of any substances which cloud or color the cocktail sample solution will minimize any color quenching.

### Procedures for Quench Correction

The loss of counts due to quenching may be corrected by several methods. One approach is the internal standard method. A sample counting rate is determined, and then a known quantity of the radionuclide of interest from a calibrated standard solution is added and the sample recounted. The counting efficiency may then be calculated by Equation 7 (So80; p. 255). Where STD is the standard sample.

$$\text{EFF} = \frac{\text{cpm (STD + sample)} - \text{cpm (sample)}}{\mu \text{ C i standard}} \quad (7)$$

Using the calculated efficiency, the activity of the sample is obtained from Equation 8.

$$\mu \text{Ci sample} = \frac{\text{cpm sample}}{\text{EFF}} \quad (8)$$

The internal standardization method is not accurate if the sample and standard are not in the same form of the labeled molecule, or if they are not dissolved in the same manner in the scintillator.

A second method of quench correction is the channels ratio method. In this method one channel is set to count an unquenched sample as efficiently as possible, and another channel to count in the energy region below the sample. The *channels ratio* is the ratio of counts of the sample to the counts in the lower-energy region. Next, a series of standards of known activity are counted, with each quenched slightly more than the proceeding sample. A quench curve may then be constructed by plotting the counting efficiency (cpm/ $\mu\text{Ci}$ ) versus the channels ratio. The advantage of the channels ratio method is that it corrects for all types of quenching. The disadvantage, however, is that at low counting rates, the statistical error in the channels ratio may be large enough to cause significant

errors in the estimated quench correction factor. Increasing the sample counting time may minimize this error (Co77; p. 92).

The automatic external standardization (AES) method is a third type of quench correction. This method incorporates features from both of the previous methods. An unquenched sample of known activity is counted, and then an external standard  $\gamma$ -ray source is automatically placed next to the vial and the sample recounted. The  $\gamma$ -rays interact with the scintillator producing Compton recoil electrons which are counted in two channels. The two channels are used as a channels ratio. Alternately, the AES ratio may be calculated using Equation 9, where *sam* is the unknown sample and STD the standard sample (So80; p. 256).

$$\text{AES ratio} = \frac{\text{cpm (sam + STD)} - \text{cpm (sam ch. 2)}}{\text{cpm (sam + STD)} - \text{cpm (sam ch. 1)}} \quad (9)$$

A series of quenched standards of known amounts of the radionuclide of interest is counted and the efficiencies related to the AES ratio. These data can then be applied to all samples to correct for quenching. The advantages of the AES method are relatively small statistical errors and sensitivity equivalent to that of the channels ratio method. However, AES only corrects for chemical and color quenching.

## HARDWARE AND ACCESSORIES

The major components of a classical LSC are the photomultiplier tubes, preamplifiers, coincidence gate, pulse summation circuit, amplifier(s), single channel analyzer (SCA -- generally three are used), a scaler for each SCA, and a readout device. Figure 7 is a schematic of the typical components and layout of a SCA-based liquid scintillation detector.

The photomultiplier tube (PMT) is the initial sensing device in the detection and processing of scintillation photons. The purpose of the PMT is to convert light energy from

the scintillant into an easily manipulated and measured electrical signals proportional in magnitude to the detected light pulse intensity. The PMT is constructed of three main parts; the photocathode, a series of dynodes, and an anode. The detector end of the PM tube is constructed of glass (or quartz, if energy in the ultraviolet range is to be detected) with a thin coating of photocathode material on the inner face of the tube. The light sensitive material of the photocathode converts light photons from the solute into electrons referred to as photoelectrons. The photocathode is constructed of a material which requires a very small amount of energy to release a photoelectron. Currently photocathodes are constructed of either cesium-antimony ( $\text{Cs}_3\text{Sb}$ ), multi-alkali or tri-alkali ( $\text{CsNa}_2\text{KSb}$ ), or bi-alkali ( $\text{K}_2\text{CsSb}$ ) materials.

Generally, the energy necessary to release a photoelectron from the photocathode is provided by the impinging scintillation photons. Energy in the form of heat (radiation of a slightly longer wavelength than light) may also cause a photoelectron to be emitted from the photocathode and detected by the PMT. These emissions are called thermionic or Joule-Thompson noise (also referred to as the *dark current* of the PMT) and may reach a level of  $10^4$  counts/minute (Ho74; p. 88). Cooling the system decreases, but will not eliminate thermionic noise. Using two PMTs simultaneously, and routing their output signals through an electronic device called a coincidence gate, can further minimize dark current problems. This is possible since thermally generated emissions are random with time and would not likely occur at the same time in both tubes, while photocathode response to scintillator photons would be detected by both tubes at almost the same instant. Hence, a coincidence gate is used, which allows further processing of signals received from both PMTs only when within  $\pm 10$  nanoseconds of each other, while discarding separately received signals. The rate of random coincidences  $R_r$  (in counts per second) accepted as a true event by the coincidence circuit can be determined by Equation 10, where  $2\tau$  is the resolving time of the circuit, and  $R_n$  is the PMT noise pulse rate (assumed to be equal in

SCHEMATIC OF A LIQUID SCINTILLATION COUNTER

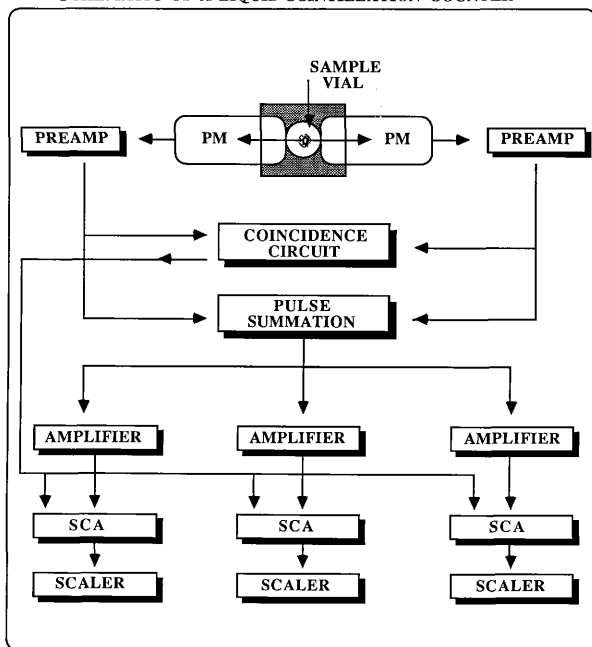


FIGURE 7: BASIC COMPONENTS OF A LIQUID SCINTILLATION COUNTER.

both tubes).

$$R_r = (2\tau)R_n^2 \quad (10)$$

The photocathode efficiency is a function of the photon wavelength and also varies over the face of the PM tube. Energy losses at this stage are due to reflection, photon energy absorption within the photocathode material without formation of a photoelectron, electrons which overcome and escape the potential barrier, and electron collisional energy losses between the photocathode and the first dynode. Photoelectrons are accelerated toward the first dynode by the potential between the dynode and the photocathode (approximately 100 to 200 volts). A series of negatively charged focusing rings act as a funnel toward the first dynode, and thus ensure that all (or at least most) of the photoelectrons reach the dynode. The dynode is also covered with photocathode material, hence, as a high-energy electron strikes the first dynode from three to five electrons are produced. Two types of dynode layouts -- linear (see Figure 8) or venetian blind -- are commonly used. The exact electron yield at the first dynode depends on the kinetic energy of the photoelectron and the work function of the dynode material. Each of these electrons is accelerated toward the next dynode by a potential difference between the two dynodes, subsequently "multiplied" and accelerated to the next dynode. From one initial electron, the dynode cascade results in approximately  $10^6$  electrons reaching the last dynode in about  $10^{-9}$  seconds. When an electron strikes the first dynode there is a reduction in potential between the dynode and the photocathode, thus when a second photoelectron strikes the first dynode it has insufficient kinetic energy for multiplication. Therefore, a second photoelectron will not be "accepted" by the first dynode until the previous cascade of electrons has traversed the tube. Photoelectrons striking the first dynode during this time are not detected. The time during which an electron cannot be accepted by the dynode is

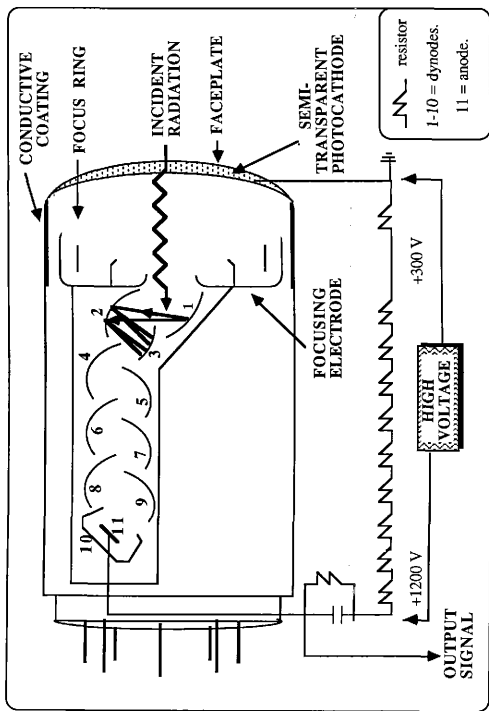


FIGURE 8: BASIC CONSTRUCTION OF A LINEAR TYPE PHOTOMULTIPLIER TUBE.

referred to as the "dead time" of the detector. The dead time of the LSC detection process, however, is relatively negligible due to the rapid speed with which a series of electrons traverse the dynode array.

The PM tube gain is the factor by which a single photoelectron is increased through the complete dynode cascade to the anode. Thus, if the average number of electrons produced at each dynode per incident electron were four, the gain would be approximately  $10^6$ . If the number of electrons were only three, however, the gain is then approximately  $5.9 \times 10^4$  -- almost one and a half orders of magnitude less. If one considers the statistical fluctuations in electron production at the first two dynodes, it becomes readily apparent that the overall fluctuations in gain are quite significant. Increasing the high voltage to the PM tube, and the resulting increase in potential between dynodes, increases the kinetic energy of transient electrons, and therefore increases the gain. Similarly, decreasing the high voltage decreases the gain. Output signal magnitude from PM tubes is strongly high voltage dependent.

The anode collects electrons from the last dynode and produces a voltage pulse. The PMT response is determined by the anode current capacity. High count rates or high-energy particles can saturate the anode and cause a nonlinear response and decreased gain. The PM tube response will eventually level out and reach equilibrium (i.e. the gain will stop shifting) at the higher counting rate in a matter of a few minutes to a few days depending on the individual tube.

The voltage output from a typical PMT is of relatively small amplitude, and therefore is generally routed through a preamplifier. The preamplifier has three main functions:

- (1) To amplify the PM tube signal as needed.
- (2) To match the impedance levels between PMT and subsequent components.
- (3) To shape the pulse for optimal processing.

The ratio of output to input amplitude, or the gain factor of the preamplifier, is generally 5 to



20 in LSCs. Signals from the preamplifier are then routed through coincidence and pulse summation circuits which correct for the PMT dark current as previously discussed.

Signals that pass through the coincidence gate are sent through a summing amplifier which reshapes the pulse from the preamplifier into a sharp peak. Amplifier gain ranges from 1 to 1000 and generally may be modified by both a coarse gain adjustment (steps of x2, x4, x8, etc.) and a fine gain adjustment which acts continuously between the coarse gain steps.

For the older design LSC systems the summing amplifier output is fed simultaneously into two or three single-channel pulse height analyzers (SCA). A SCA has operator-set upper (ULD) and lower level (LLD) discriminators. The combined circuits for the discriminators, ULD, and LLD is often called a single channel analyzer (SCA). Pulse heights above the ULD or below the LLD will be ignored by the discriminator, while pulses within the limits will be summed and counted. At this point, one should recall that the pulse height fed to the discriminator is a function of the amplifier (and preamplifier) pulse, which was in turn a function of the integrated intensity of scintillation events seen by the PM tube, and thus the pulse height is in direct proportion to the  $\beta$  energy characteristic of the nuclide decay in the sample. Each discriminator output is then channeled into a separate *scaler*. The scaler simply tallies each pulse passing the discriminator. In this method the pulses are divided into separate 'windows' representative of the pulse height range determined by the ULD and LLD settings.

Although the multichannel analyzer (MCA) has not, until now, been commonly used in conjunction with LSC's, a discussion of their function will be included here since the detector used for this research utilizes a MCA. Some applications of pulse-height analysis require simultaneous recording of events in multiple energy windows. Although multiple SCAs could be implemented for such jobs, the SCA expense and difficulties encountered in proper window adjustments are prohibitive. Figure 9 indicates how an MCA can be

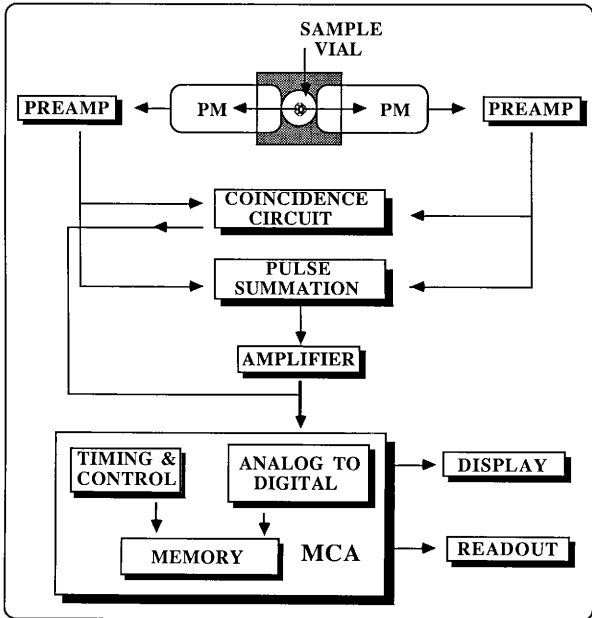


FIGURE 9: SCHEMATIC OF A LSC WITH ATTACHED MCA.

incorporated into a LSC. A MCA typically is composed of an analog-to-digital converter (ADC), memory, timing and control circuits, readout and display devices.

Pulses from the amplifier are fed into the ADC, which sorts the incoming pulses into a finite number of intervals or *channels* according to the pulse amplitude. The ADC may divide the typical 0 to 10 volt amplifier pulse range into anywhere from 100 channels in a small MCA, to 8192 channels in a very large MCA. The first channel in a 1000 channel MCA, for example, would correspond to the 0.01 to 0.02 volt range of pulses from the amplifier, etc. Figure 10 shows the basic principle of the ADC. The most common ADC used is a ramp converter. The ramp converter deposits an input pulse from the amplifier as a charge on a capacitor proportional to the pulse amplitude (or energy). The capacitor then discharges through a resistor, thereby forming a *gate pulse*, and activating a *clock oscillator*.

The clock oscillator produces a series of pulses which are recorded in a counting circuit as long as the capacitor is discharging. When the capacitor is fully discharged, the clock oscillator is turned off and the number of clock pulses is tallied. The total number of clock pulses corresponds to the initial amount of energy deposited on the capacitor, and thus to the energy of the incoming pulse. The memory channel corresponding to the appropriate number of clock pulses can then be incremented by one count, and the input circuitry cleared to accept the next incoming pulse. Thus the ADC converts the analog signal (volts of pulse amplitude), into a digital signal (channel number). Data from each ADC channel is then passed to a unique memory location in the MCA. The display or printout device can then construct a pulse-height spectrum which shows a spectrum of counts versus channel number from the data stored in the various memory locations. It should be noted that the channel number also corresponds to a specific energy range deposited in the detector by the beta particle.

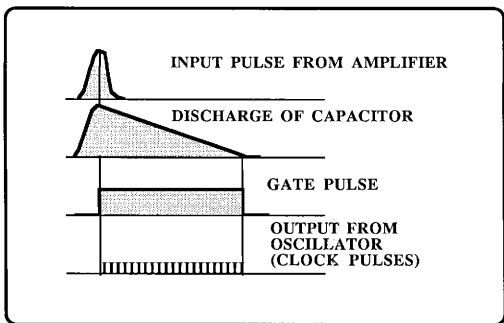


FIGURE 10: BASIC PRINCIPLES OF AN ANALOG-TO-DIGITAL CONVERTER.

#### Counting Vials and Sample Preparation

Samples are placed in vials of the appropriate size to fit in the counting chamber of the individual LSC. Counting vials are generally constructed of polyethylene or low-potassium-content glass. The naturally radioactive potassium-40 content in standard glass, which is not low-potassium, can increase the background count by 30 to 40 counts per minute (So80; p. 251). Polyethylene vials may distort or swell when used with toluene or similar aromatic solvents, but are suitable for use with dioxane solvents.

A complete discussion of sample preparation techniques is beyond the scope of this document. In sample preparation, however, one must consider a number of items:

- (1) Sample solubility
- (2) All types of quenching
- (3) The effect of the sample on solute solubility
- (4) Sample or solute precipitation

- (5) Sample or scintillant interaction with counting vial, and
- (6) Emulsions (can cause quenching)

Each of these subject is thoroughly discussed in Applications of Liquid Scintillation Counting, chapter 6, by Horrocks (Ho74).

## EQUIPMENT AND PROCEDURES

### THE LIQUID SCINTILLATION SPECTROMETER

The LKB-Wallac 1219 Rackbeta 'Spectral' liquid scintillation spectrometer (Spectral) is designed to count all types of beta emitting samples over the energy range of 1 to 2000 keV. Several unique features are included which allow a more complete determination of radionuclide samples than was previously possible (refer to Figure 11 for schematic). The incorporated multi-channel analyzer (MCA) is responsible for the wide energy range, a spectrum display divided into 1024 channels, and highly precise quench monitoring. The LKB-Wallac method of Automatic Continuous Spectrum Stabilization (ACSS -- discussed below) continuously calibrates the instrument gain. Operational control is through an AT&T PC 6300 micro-computer, associated video monitor, and "Multicapture" software package (supplied by LKB). Appendix A can be referred to for a diagram of the Spectral's operational flow chart (LKB87b).

Up to 300 samples in standard 20 ml vials or 660 samples in 15-18 ml miniature vials can be automatically counted. Standard low potassium 20 ml glass vials were used for this research. Consecutive racks of 10 sample vials are placed on a rubber conveyor belt in two arrays of 15 racks each under a protective plastic cover. Code plugs placed on the racks initiate count parameter selection or automatic counting shut down, allow multi-user capabilities, and provide for positive sample identification. Electro-optical sensors detect rack position, read code plugs, and activate the sample lifting mechanism. The optional cooling unit was not included in the unit used for this research.

The lead shielded detector assembly is at the back of the conveyor belt, and high enough to allow sample rack clearance between the detector unit and the conveyor. The measurement chamber is centered between two high-speed, low-noise PM tubes with attached pre-amplifiers. The microprocessor, memory, counting, pulse height discrim-

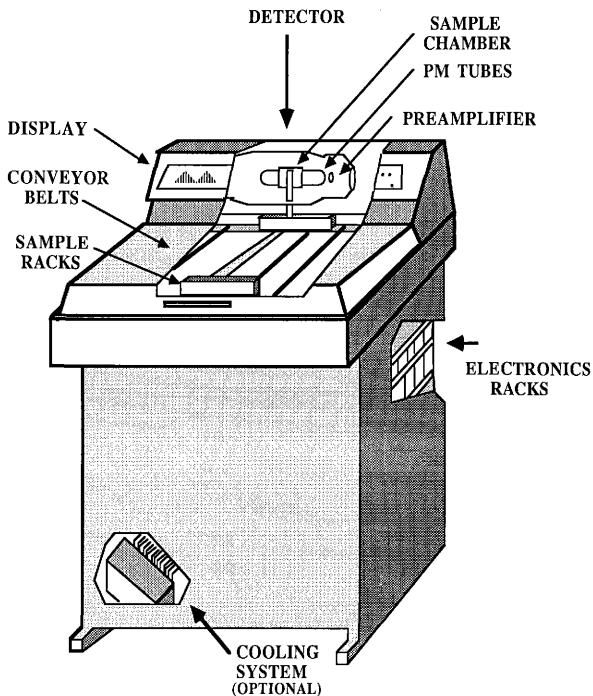


FIGURE 11: LAYOUT OF THE LKB-WALLAC 1219 RACKBETA 'SPECTRAL' LIQUID SCINTILLATION SPECTROMETER

ination circuits, and power supply are incorporated into printed circuit boards on an electronics rack located below the conveyor.

The inclusion of a 1024-channel multi-channel analyzer (MCA) is the primary advantage of the Spectral over conventional LSCs. Use of an MCA allows counting with precise and variable window settings over a large energy range. The low energy region is "expanded" due to the logarithmic energy scale (400 channels cover the tritium spectrum). Highly precise chemiluminescence and automatic quench correction are provided. Linear amplification of detector data is followed by a logarithmic analog-to-digital conversion (ADC), thus more precise window settings at low energies are possible. The ADC includes a timing circuit for automatic dead-time correction. Dead-time correction has been shown to be effective even at counting rates greater than  $10^6$  cpm (Mc87).

Spectrum drift due to PM tube and high voltage supply instabilities is corrected for by the Automatic Continuous Spectrum Stabilization (ACSS). A light emitting diode is on a low duty cycle to form a constant intensity light pulse which is seen by the detector and compared through a feedback circuit to a reference pulse for calibration purposes. If the diode pulse is larger than the reference, the PM tube high voltage is decreased. If lower, the high voltage is increased. This sequence is repeated 62 times per second so that an effectively constant detector gain is achieved. The ACSS advantages are:

- 1) Continuous stability and calibration
- 2) Precise and reproducible count windows
- 3) Automatic compensation for PM tube and component ageing
- 4) Reproducible count results
- 5) Immediate  $\pm 0.2$  % stability with no warm up period
- 6) Lengthened PM tube life
- 7) A simple and reliable sample lifting mechanism can be utilized.



Conventional LSCs require a constant, continuous PMT high voltage to ensure detector gain stability. Consequently, a double shutter mechanism is essential to keep light out of the measurement chamber during sample transit. Since the ACSS ensures stability in the Spectral, the PM tube high voltage may be interrupted while the sample is inserted or removed from the counting chamber. Thus, a simple single-shutter measurement chamber can be utilized. A plug on the elevator mechanism that raises the sample forms a light tight seal to the counting chamber. Optical sensors switch off the high voltage to the PM tubes when the sample mechanism is actuated.

Several quench standardization methods are available in the Spectral. Single sample methods involve the addition (either manually or automatically) of a quenching agent with spectra recorded between each addition. These data are used to form a quench curve. Alternately a sample series with incremental quenching can be counted to construct a quenching curve. Quench curves entered into the Spectral memory may be used for automatic correction of sample quenching and for calculation of disintegration per minute values.

The delayed coincidence method is employed to monitor the count rate due to random incidents. The Spectral automatically displays the percentage of the total counts that is due to random coincidences. Static electric discharge monitoring is also automatic. The total counting period is divided into incremental units and monitored for any statistically significant change.

Display units on the front of the Spectral show both numerical data and spectra on a fluorescent dot matrix (256 columns and 64 rows). Alternately, information and spectra may be displayed on the video monitor, printed out as hard copy, or stored as files on computer disk.

## EXPERIMENTAL PROCEDURES

### General Practices

Throughout this investigation, care was taken to avoid any possible inadvertent contamination of samples. All samples were numbered and the content recorded. Cocktail was dispensed directly from the cocktail container with no contact between the dispenser and sample vials. New, low-potassium glass sample vials were obtained, and were not reused. Disposable pipets from sealed packets were used for all large volume solution transfers. Automatic micro-pipets with disposable tips were used for all small volume transfers. A new pipet, or pipet tip was used for each solution transfer. To minimize possible impurity inclusions, caps were kept on samples at all times and removed only as necessary to add solutions. All cocktail solutions were stored in a drawer to minimize exposure to light and resultant chemiluminescence problems. For consistency, a one minute counting time was used on all samples in the study.

### Liquid Scintillation Cocktail

Liquid scintillation cocktail (henceforth referred to as cocktail) was obtained from and prepared at the Texas A&M University Radiological Safety Office (RSO). To help keep background counts at a minimum, cocktail was stored in a glass jug wrapped with black tape to avoid light induced phosphorescence events in the cocktail. The cocktail consisted of 1125 mL of meta-, ortho-, and para-xylene (primarily meta-xylene), in which were dissolved 4.5 g 2,5-diphenyloxazole (PPO) solute, and 375 mL octylphenoxypolyethoxy-ethanol (Triton X-100 brand) surfactant. The light output of xylene and PPO, relative to other common solvents and solutes, is 97 % and 100 % respectively.

### Standard Spectra

Periodically throughout the research a vial with 15 mL of pure cocktail was counted on the Spectral to obtain background variation data. A typical background spectrum is included in the spectra catalogue.

The most commonly used radioisotopes at the Texas A&M Campus are  $^{32}\text{P}$ ,  $^{35}\text{S}$ ,  $^{45}\text{Ca}$ ,  $^3\text{H}$ ,  $^{125}\text{I}$ , and  $^{14}\text{C}$ . The radionuclides directly involved in the regulatory change were  $^3\text{H}$ ,  $^{125}\text{I}$ , and  $^{14}\text{C}$ . Procedural controls (asking researchers to keep isotopes separated, etc.) can reasonably be expected to keep isotopes mixtures to two or less nuclides per sample in university or medical situations. Thus it was decided that the radionuclide mixtures (with two isotopes at the most in each sample) of primary interest were:

- 1) Small amounts of  $^{32}\text{P}$ ,  $^{35}\text{S}$ ,  $^{45}\text{Ca}$ , and  $^{125}\text{I}$  in varying ratio to  $^3\text{H}$
- 2) Small amounts of  $^{32}\text{P}$ ,  $^{35}\text{S}$ ,  $^{45}\text{Ca}$ , and  $^{125}\text{I}$  in varying ratio to  $^{14}\text{C}$
- 3) Small amounts of  $^{32}\text{P}$ ,  $^{35}\text{S}$ ,  $^{45}\text{Ca}$  in varying ratios to  $\text{I}^{125}$

Individual samples of  $^{32}\text{P}$ ,  $^{35}\text{S}$ ,  $^{45}\text{Ca}$ ,  $^3\text{H}$ ,  $^{125}\text{I}$ , and  $^{14}\text{C}$  were obtained from various laboratories on the Texas A&M campus. Only the approximate sample activity of each was known. Table 4 shows the amounts acquired.

### Sample Spectra

The  $^{32}\text{P}$ ,  $^{35}\text{S}$ ,  $^{45}\text{Ca}$ , and  $^{125}\text{I}$  samples were diluted with cocktail to 15 mL total volume. Rough calculations were made to determine the portion of each necessary to yield stock solutions of individual nuclides with approximately  $1.0 \times 10^6$  counts per minute (cpm) each. The calculated amount for each radionuclide was pipetted into a separate labeled 20 mL glass scintillation vial. The stock solutions were completed by addition of sufficient cocktail to bring the total sample volume in each vial to 15 mL. The CPM and spectra of

TABLE 4. SAMPLE RADIOISOTOPE ACQUISITION, ACTIVITY, AND VOLUME DATA.

Isotope	Origin	Approximate Activity	Approximate Volume
P-32	Biochemistry	10 $\mu$ Ci	1 $\mu$ L
S-35	Biochemistry	10 $\mu$ Ci	1 $\mu$ L
H-3	RSO	3 $\mu$ Ci	4 mL
C-14	RSO	5 $\mu$ Ci	10 mL
Ca-45	Oceanography	2 $\mu$ Ci	100 $\mu$ L
I-125	Oceanography	2 $\mu$ Ci	100 $\mu$ L

each was then determined on the Spectral. These reference spectra were saved to be used as a catalogue of pure isotopes. A rough quench check was made by comparing these spectra to reference spectra of  $^{14}\text{C}$  and  $^3\text{H}$  standard samples provided by LKB-Wallac. Since the spectrum of all samples was recorded over the full range of channels (5-1024), small amounts of quenching had negligible effect and resulted in no loss of counts. Furthermore, the development of better scintillation cocktails, and increased PM tube response has allowed minor variations in sample volume with no effect on counting efficiency (LKB87c).

Using  $^{32}\text{P}$  in tritium as an example, the procedure shown below was used to prepare all samples, and to collect spectral data.

- (1) From stock solution, prepare vial #1 with  $\sim 2000$  cpm per 0.1 ml  $^3\text{H}$ .
- (2) Prepare  $\sim 10$  ml solution of  $\sim 2000$  cpm  $^{32}\text{P}$  in vial #2, and record spectra.
- (3) Add  $\sim 2000$  cpm  $^3\text{H}$  ( $\sim 0.1$  ml) from vial #1 into vial #2, and record spectrum.
- (4) Repeat step 4 until a cpm of  $\sim 20,000$  is reached.
- (5) Add  $\sim 4000$  cpm  $^3\text{H}$  (0.2 ml) from vial #1 into vial #2, and record spectrum.

- (6) Repeat step 5 until a cpm of ~100,000 is obtained.

These spectra represent  $^{32}\text{P} : ^3\text{H}$  ratios of approximately 1:1, 1:2, 1:3, 1:4, 1:5, ... , 1:10, and 1:12, 1:14, 1:16, ... , 1:50. The above procedure was repeated with the appropriate nuclide combinations to obtain ratios for each of the desired mixtures. All sample spectra were printed out and filed for later use in unknown sample determinations.

#### Data Manipulation

All spectra were uploaded from an IBM-PC computer into the Engineering Services Center VAX 8000 series, VMS 4.6 system computer. Spectra were then edited to leave paired data sets, consisting of the channel number and recorded cpm values for X and Y coordinates, respectively. A Fortran code, 'ZERO', was prepared which transformed data into appropriate form for logarithmic graphs. A 'Picsure Plus' package on the VAX was then used to produce representative plots for each isotope mixture, pure spectra, and background data. Several command files were prepared to facilitate graph generation. A Fortran program, 'CONVERT', was also prepared to transform some files not properly uploaded. Uploading procedures, ZERO and CONVERT programs, and command files are shown in Appendix B.

## RESULTS

### GENERAL INFORMATION

As discussed earlier, spectra for varying activities of one isotope in a constant activity of a second isotope were recorded on the Spectral. These data was then uploaded to the VAX system, and representative plots generated using the 'Picsure Plus' system package. For each graph the counts per minute was plotted as a function of isotope energy on a natural logarithmic scale (shown as channel number). It was found that in cases of a very large difference in isotope concentrations, plotting the cpm on a logarithmic scale greatly enhanced the ability to detect the lower activity radioisotope. Thus, for each sample mixture the spectra with the greatest activity difference between the two isotopes was represented in both log-log and linear-log form on one graph for comparison.

Figures 12, 13, and 14 illustrate pure isotope reference spectra (cpm on linear scale), pure spectra with cpm on a natural logarithmic scale, and typical background data, respectively. Figures 15 through 18 depict the complete set of curves for varying ratios of  $^{125}\text{I}$  in  $^{14}\text{C}$ . Figure 19 is the comparison of a linear scale cpm versus a natural logarithmic scale cpm for the 1  $^{125}\text{I}$  to 48.9  $^{14}\text{C}$  ratio. Beginning at Figure 20 and continuing through Figure 49, three graphs per isotope combination illustrate representative curves, including the cpm on a natural logarithmic scale as the third plot of each set.

### SAMPLE SPECTRA

#### Pure Spectra and Background Data

As expected, the pure spectra of all of the research isotopes are easily recognizable by their distinct shape (i.e., number and placement of peaks) and energy range (i.e., the range of channel numbers covered by the spectra) as seen in Figure 12. The reference

background spectra is shown in figure 14. It should be noted that the background addition per channel is so low as to have no significant effect on the shape of sample spectra at the activity levels used in this research. Typical one hour and one minute background counts taken over the channel range of 5 to 1024 were  $109.71 \pm 0.62$  and  $114.94 \pm 9.10$  cpm respectively. One minute background spectra are shown in Figure 14, and are important to consider since the sample spectra were taken on one minute counts. A narrow peak can be seen from channel 25 to 250, with a small amount of activity in the higher channels. This difference in counts at the higher channels is highly variable due to statistical variations and is especially noticeable when the cpm is plotted on a logarithmic scale. Care should be taken not to think that a background peak indicates an isotope when looking at a log-log plot.

#### Methods of Isotope Determination and Identification in Mixtures

Several radionuclide identification methods were considered. It should be recalled that mixtures with a maximum of two isotopes were used for this research, and the following discussion is based on this premise. The ideal method for identification and determination of radionuclides would be a curve stripping method based on the isotope peaks, or curve shape. This method, however, was not feasible for several reasons. The primary deficiency of curve stripping spectral data is the innate statistical deviations within each channel on a one minute count. Thus, curve stripping results in false data, inaccurate and unidentifiable curves, and spurious data unless the isotope concentrations are a maximum of one order of magnitude difference. At these levels, and in fact at any level, the fastest, most accurate, and simple method of isotope identification is simple visual inspection followed by comparison to the reference data generated in this research. Once the closest match to a reference curve is thus determined, the ratio of isotopes in the unknown sample may be considered to be approximately equivalent to that of the reference curve. The following discussion considers the accuracy of this method for each isotope combination.

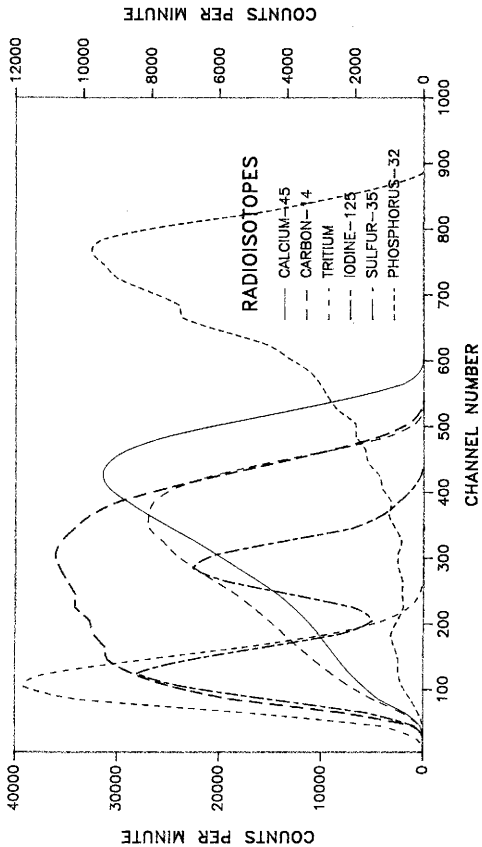


FIGURE 12: SPECTRA OF PURE RADIOISOTOPES:  
 LEFT AXIS; C-14, I-125, H-3. RIGHT AXIS; P-32, S-35, CA-45.



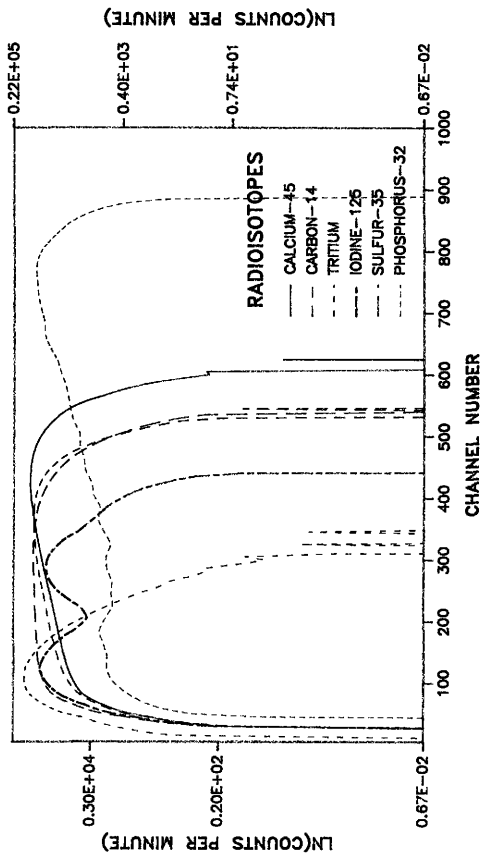


FIGURE 13: SPECTRA OF PURE RADIOISOTOPES ON A LOGARITHMIC SCALE:  
 LEFT AXIS; CA-45, H-3, C-14. RIGHT AXIS; I-125, S-35, P-32.

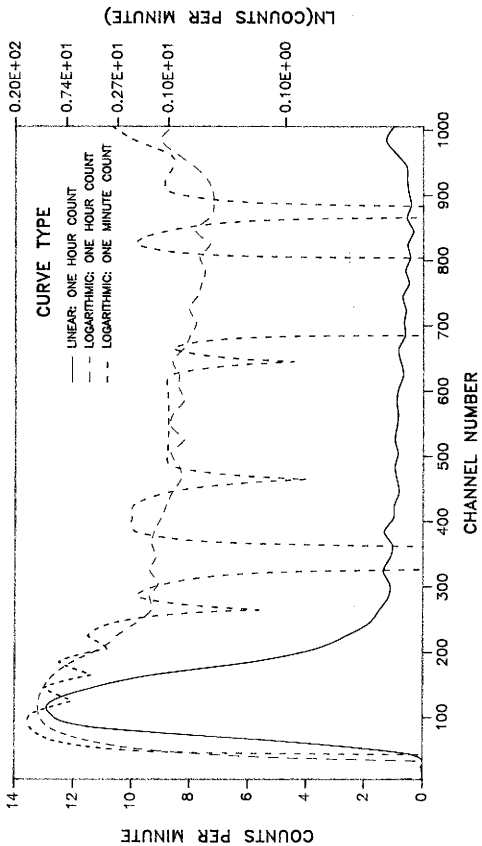


FIGURE 14: COMPARISON OF TYPICAL BACKGROUND SPECTRA ON LINEAR VERSUS LOGARITHMIC SCALES.

Spectra of  $^{14}\text{C}$  Mixtures (Figures 15-28)

$^{14}\text{C}$  has a relatively gaussian shaped distribution heavily shifted to the right. The single major peak is from channel 305 to 424. The  $^{14}\text{C}$  energy range is from channel 45 to 525.

$^{125}\text{I}$  has a bi-modal distribution with definitive peaks at channel 105 to 164, and 265 to 324. The addition of  $^{125}\text{I}$ , therefore, is easily identified visually when the ratio of  $^{125}\text{I} : ^{14}\text{C}$  is less than  $\sim 1 : 27$ . At larger ratios than this, the first  $^{125}\text{I}$  peak which is seen at the lower ratios, becomes 'covered' by the  $^{14}\text{C}$  spectra.  $^{125}\text{I}$  can often be identified at ratios above  $1 : 27$  by plotting the cpm data on a natural logarithmic scale, where the first  $^{125}\text{I}$  peak can still be seen (Figure 22). If, however, the peak on a natural logarithmic scale should fall at the top of the decade, it is very difficult to distinguish between a pure  $^{14}\text{C}$  curve, or a mixture of  $^{14}\text{C}$  and  $^{125}\text{I}$ .

$^{45}\text{Ca}$  has a gaussian shaped curve, also shifted to the right.  $^{45}\text{Ca}$  has one peak from channel 385 to 484. Although this peak is slightly to the right of a  $^{14}\text{C}$  peak, the difference is not large enough for unknown isotope identification. The energy range of  $^{45}\text{Ca}$  however, ends at channel 600, compared to channel 525 for  $^{14}\text{C}$ . Thus, any spectra which looks similar to  $^{14}\text{C}$ , but has a 'tail' out to channel 600 can be relatively easily matched to reference data even up to a 1 part  $^{45}\text{Ca}$  in 50 parts  $^{14}\text{C}$ , especially if the shoulder on the right-hand side of a natural log plot is noted.

$^{32}\text{P}$  has a very high energy beta, and therefore the primary  $^{32}\text{P}$  peak is between channels 725 and 804. Thus,  $^{32}\text{P}$  is the most easily identified contaminating isotope, and is easily seen through a 1  $^{32}\text{P}$  to 50  $^{14}\text{C}$  ratio, especially on a natural log plot.

The  $^{35}\text{S}$  peak is very broad -- stretching from channel 145 to 384.  $^{35}\text{S}$ , however, also has an energy range almost identical to the  $^{14}\text{C}$  range and thus identification is difficult. A noticeable broadening of the  $^{14}\text{C}$  peak is sufficient for  $^{35}\text{S}$  determination below a 1  $^{35}\text{S}$  to 4  $^{14}\text{C}$  ratio. Above this level the mixture cannot be differentiated from pure  $^{14}\text{C}$  without

taking a second spectra at a later date and then using the difference in half-lives to tell whether  $^{35}\text{S}$  is present in the unknown sample.

#### Spectra of $^3\text{H}$ Mixtures (Figures 29-40)

Tritium has a very narrow peak at channel 105 to 164, and is therefore the most easily differentiable isotope, in any mixture.

All of the isotope combinations have a 'tail' to the right of the  $^3\text{H}$  peak. For any of the isotopes ratios of less than 1 : 10  $^3\text{H}$  can be easily matched to the reference spectra. Above this level, the difference in energy ranges for  $^{125}\text{I}$ ,  $^{35}\text{S}$ , and  $^{45}\text{Ca}$  allow easy identification. Plotting the curves on a natural log plot yields very characteristic curves for  $^{125}\text{I}$ ,  $^{35}\text{S}$ ,  $^{32}\text{P}$ , and  $^{45}\text{Ca}$  that cannot be misinterpreted.

#### Spectra of $^{125}\text{I}$ Mixtures (Figures 41-49)

Iodine-125 mixtures are similar to  $^3\text{H}$  mixtures in that all of the research isotopes have an energy range that is significantly greater than  $^{125}\text{I}$ . Even at a 1  $^{32}\text{P}$  (or  $^{45}\text{Ca}$ , or  $^{35}\text{S}$ ) to 1  $^{125}\text{I}$  ratio, the dual peaks of the  $^{125}\text{I}$  can easily be identified. The other component of the radioisotope combination can be determined by energy range differences. Again similar to  $^3\text{H}$  mixtures, the curves are even more precise on a natural log scale.

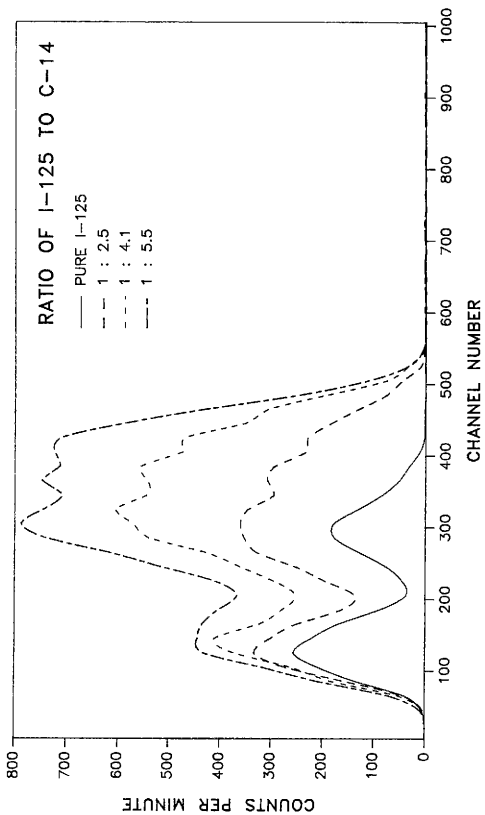


FIGURE 15: IODINE-125 IN VARYING AMOUNTS OF CARBON-14;  
RATIOS FROM PURE I-125 TO 1 : 5.5.

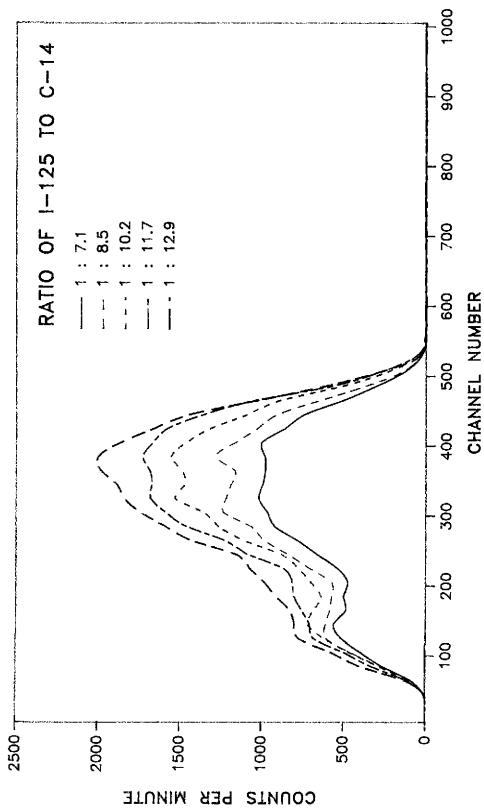


FIGURE 16: IODINE-125 IN VARYING AMOUNTS OF CARBON-14;  
RATIOS FROM 1 : 7.1 TO 1 : 12.9.

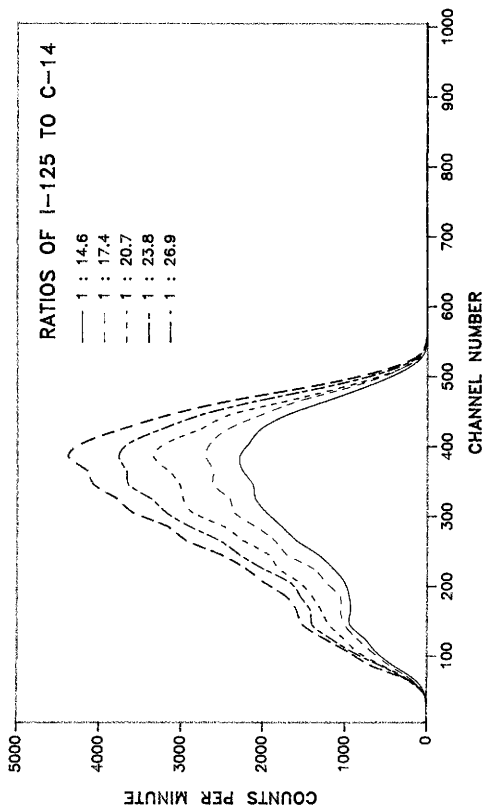


FIGURE 17: IODINE-125 IN VARYING AMOUNTS OF CARBON-14;  
RATIOS FROM 1 : 14.6 TO 1 : 26.9.

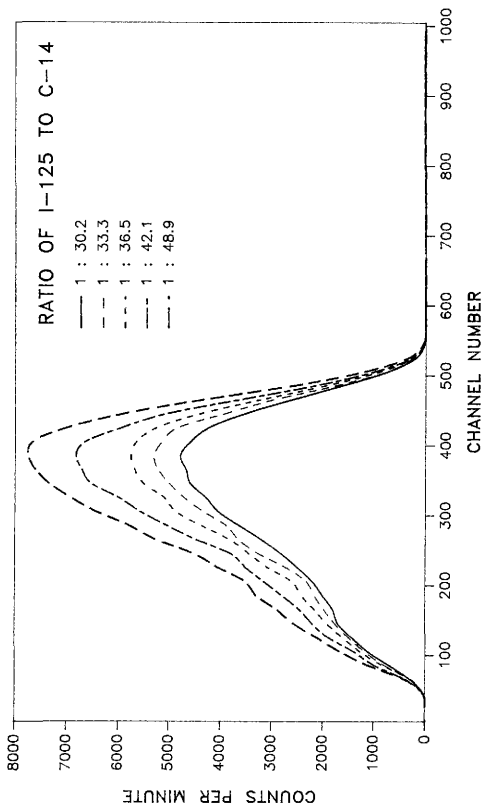


FIGURE 18: IODINE-125 IN VARYING AMOUNTS OF CARBON-14;  
RATIOS FROM 1 : 30.2 TO 1 : 48.9.



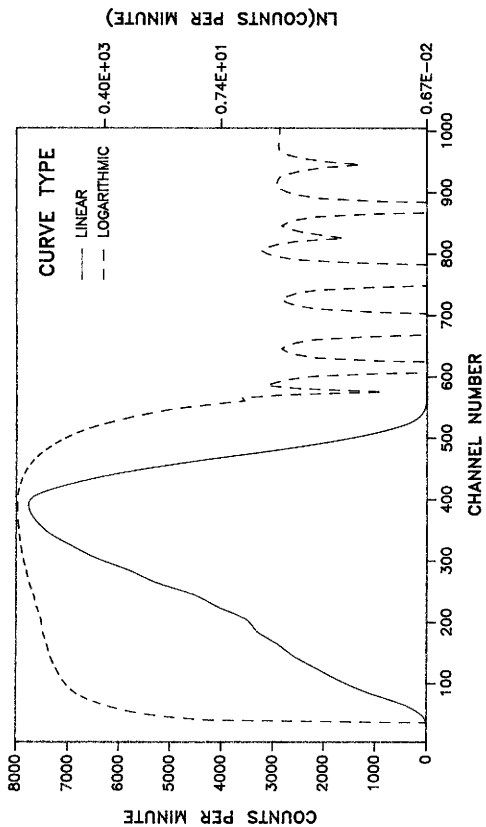


FIGURE 19: COMPARISON OF 1 IODINE-125 TO 48.9 CARBON-14 ON LINEAR VERSUS LOGARITHMIC SCALES.

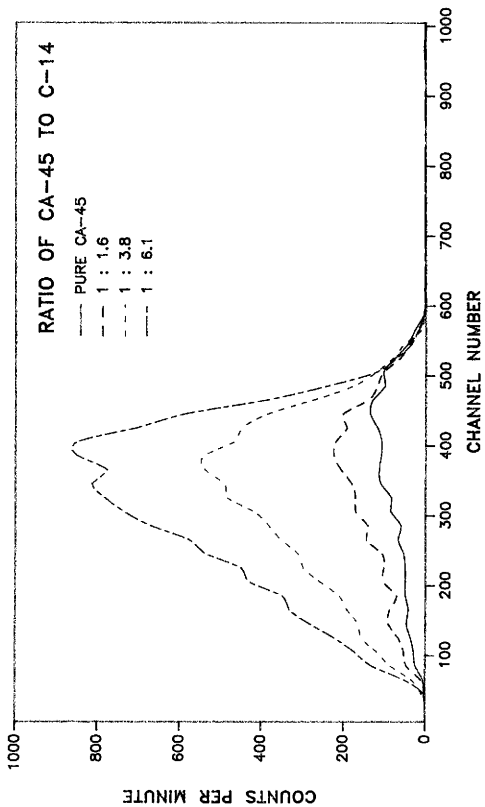


FIGURE 20: CALCIUM-45 IN VARYING AMOUNTS OF CARBON-14;  
 RATIOS FROM PURE CALCIUM-45 TO 1 : 6.1.

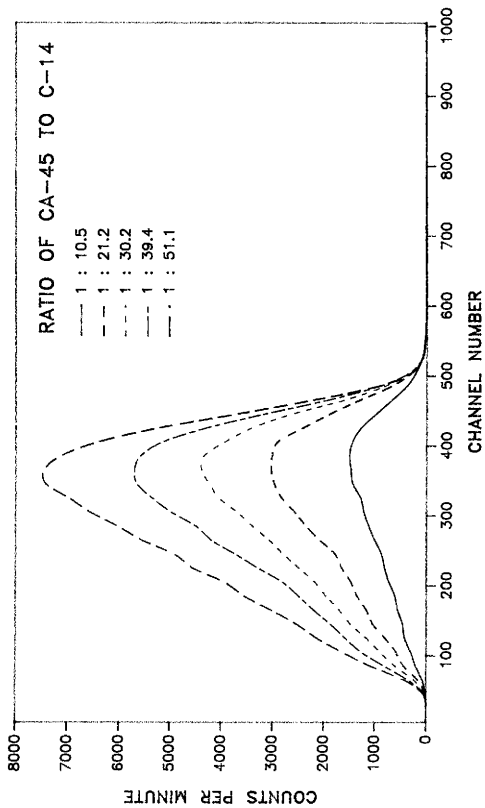


FIGURE 21: CALCIUM-45 IN VARYING AMOUNTS OF CARBON-14;  
RATIOS FROM 1 : 10.5 TO 1 : 51.1.

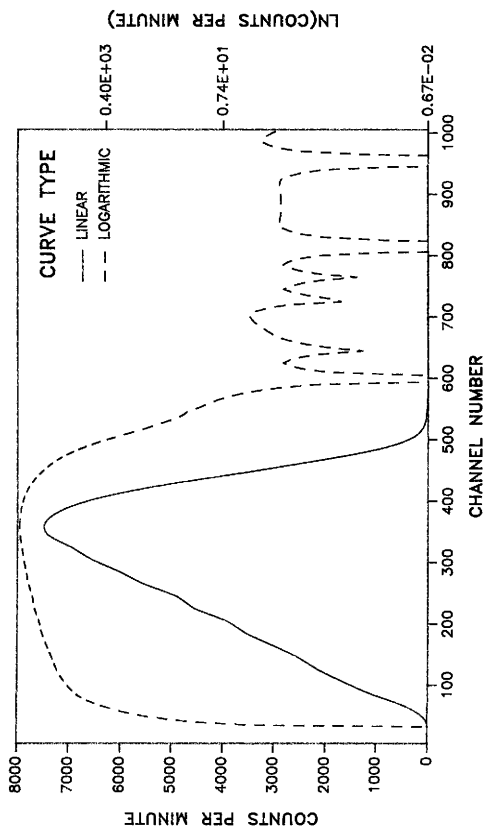
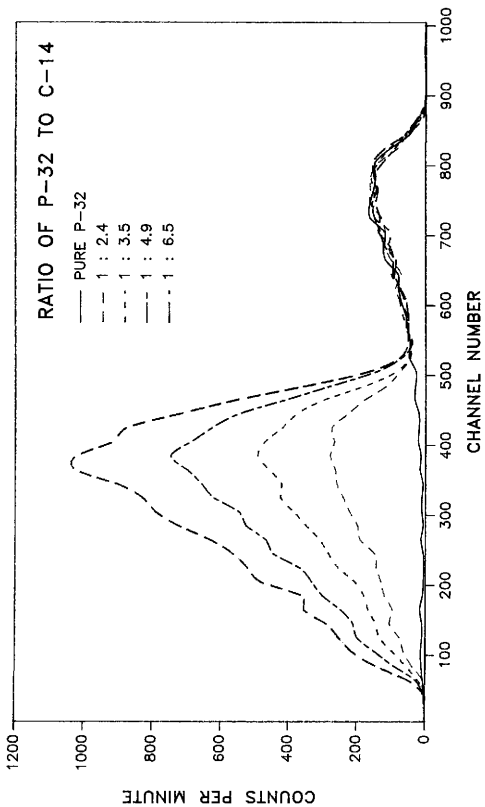
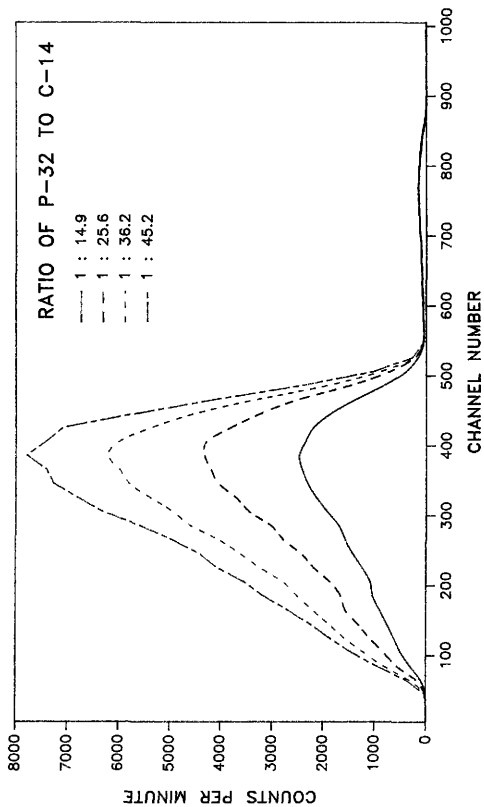


FIGURE 22: COMPARISON OF 1 CALCIUM-45 TO 51.1 CARBON-14 ON LINEAR VERSUS LOGARITHMIC SCALES.



**FIGURE 23: PHOSPHORUS-32 IN VARYING AMOUNTS OF CARBON-14;  
RATIOS FROM PURE P-32 TO 1 : 6.5.**



**FIGURE 24: PHOSPHORUS-32 IN VARYING AMOUNTS OF CARBON-14;  
RATIOS FROM 1 : 14.9 TO 1 : 45.2.**

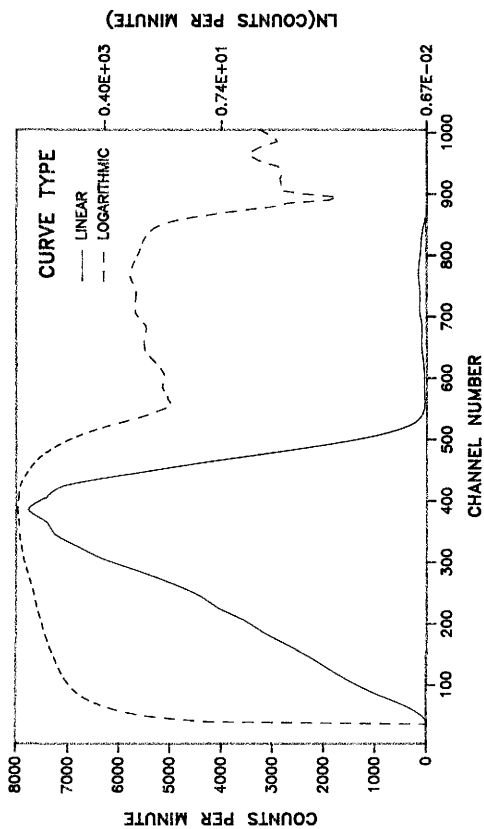
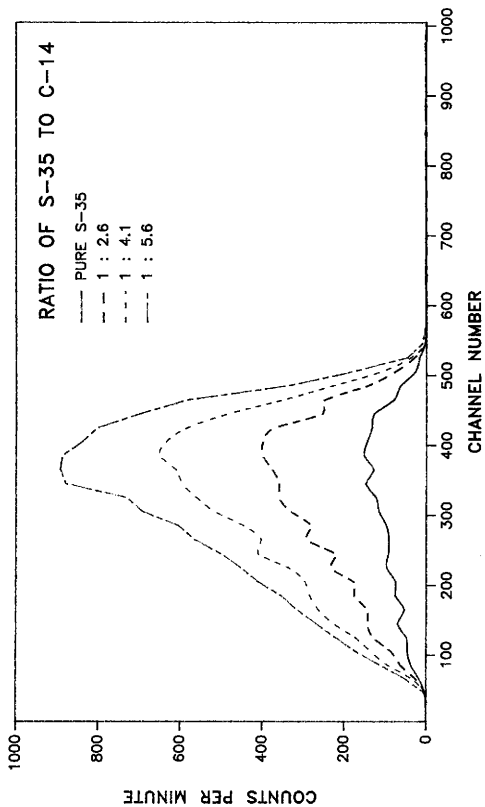
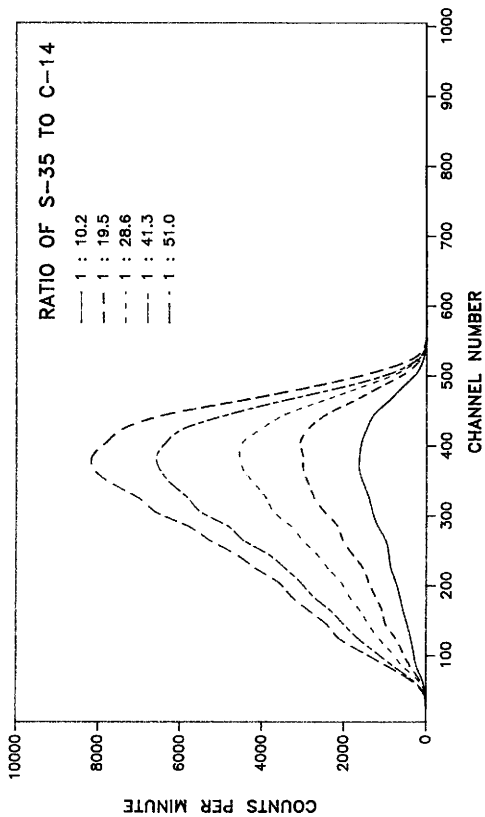


FIGURE 25: COMPARISON OF  $^{32}\text{P}$  TO  $^{45.2}\text{Ca}$  ON LINEAR VERSUS LOGARITHMIC SCALES.



**FIGURE 26: SULFUR-35 IN VARYING AMOUNTS OF CARBON-14;  
RATIOS FROM PURE S-35 TO 1 : 5.6.**





**FIGURE 27: SULFUR-35 IN VARYING AMOUNTS OF CARBON-14; RATIOS FROM 1 : 10.2 TO 1 : 51.0.**

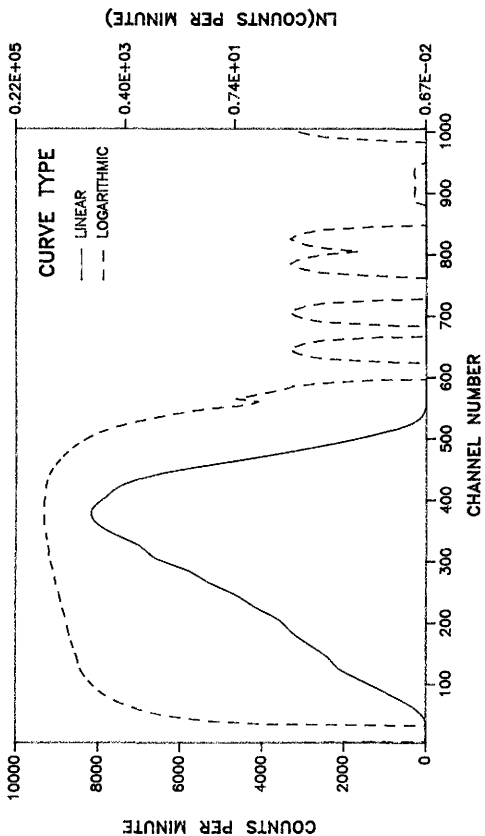
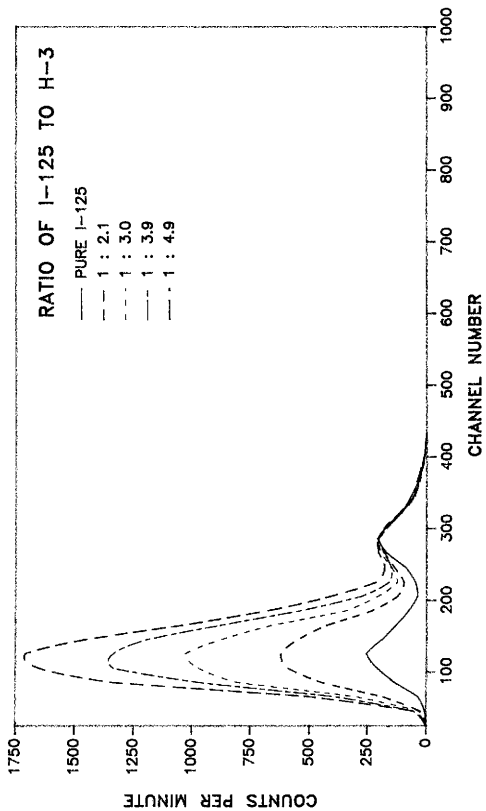


FIGURE 28: COMPARISON OF 1 SULFUR-35 TO 51.0 CARBON-14 ON LINEAR VERSUS LOGARITHMIC SCALES.



**FIGURE 29: IODINE-125 IN VARYING AMOUNTS OF TRITIUM;  
RATIOS FROM PURE I-125 TO 1 : 4.9.**

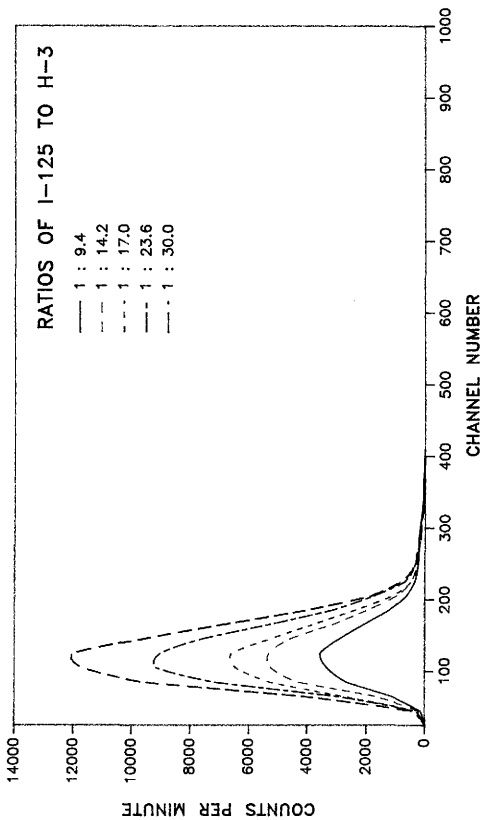


FIGURE 30: IODINE-125 IN VARYING AMOUNTS OF TRITIUM;  
RATIOS FROM 1 : 9.4 TO 1 : 30.

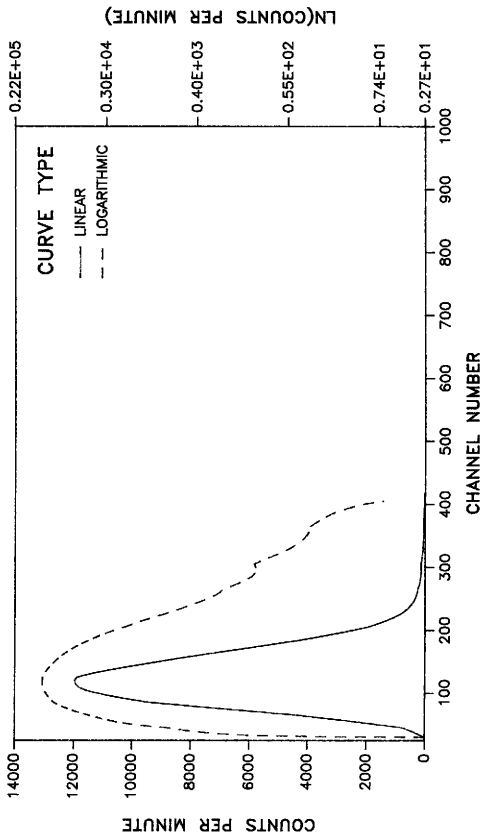
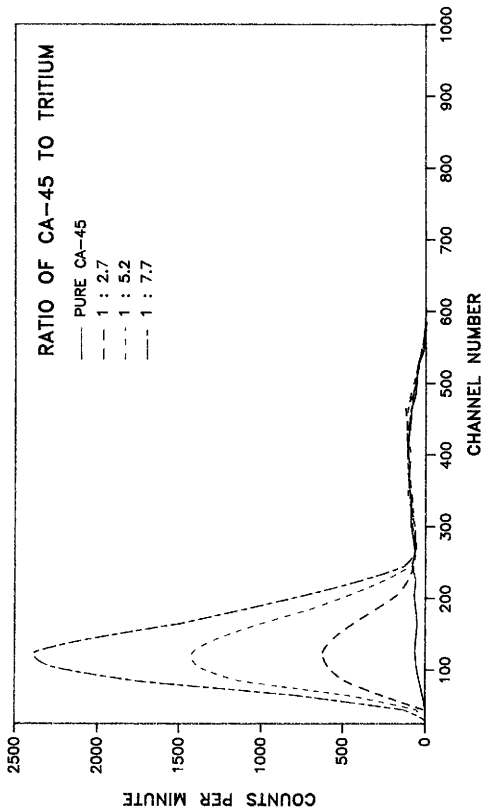
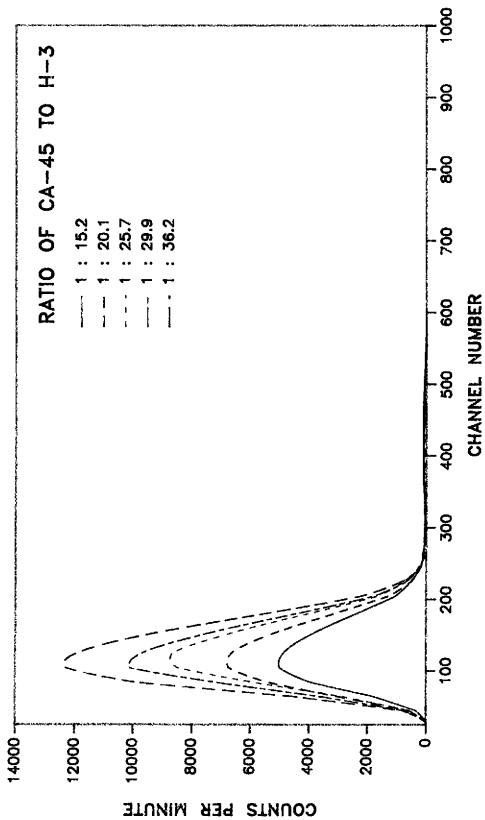


FIGURE 31: COMPARISON OF 1 IODINE-125 TO 30.0 TRITIUM ON LINEAR VERSUS LOGARITHMIC SCALES.



**FIGURE 32: CALCIUM-45 IN VARYING AMOUNTS OF TRITIUM;  
RATIOS FROM PURE CA-45 TO 1 : 7.7.**



**FIGURE 33: CALCIUM-45 IN VARYING AMOUNTS OF TRITIUM; RATIOS FROM 1 : 15.2 TO 1 : 36.2.**

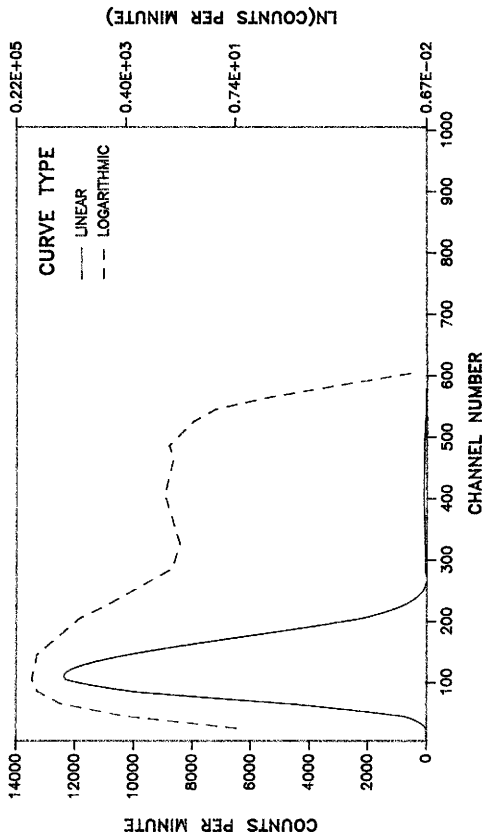
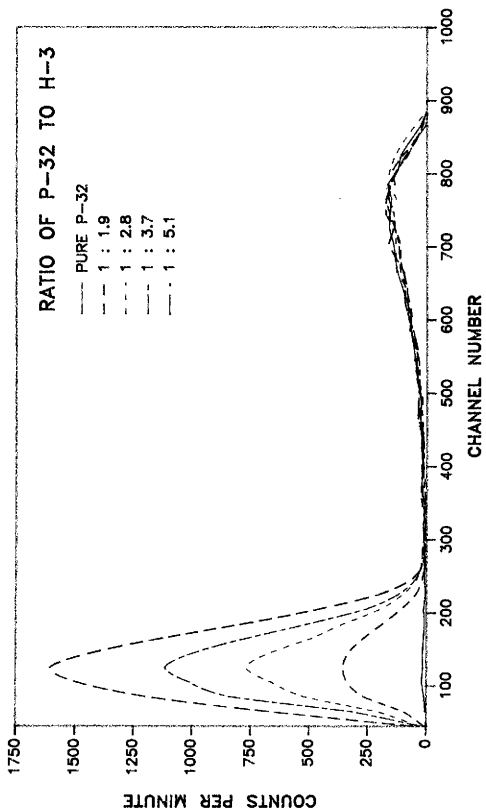
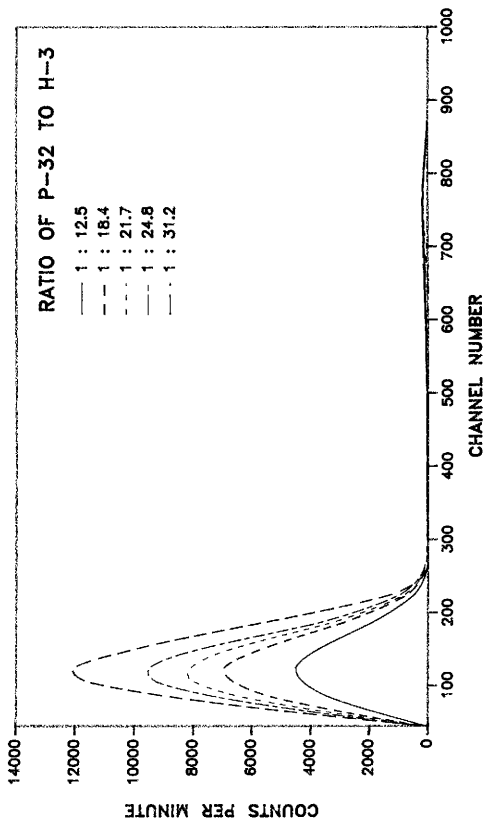


FIGURE 34: COMPARISON OF 1 CALCIUM-45 TO 36.2 TRITIUM ON LINEAR VERSUS LOGARITHMIC SCALES.





**FIGURE 35: PHOSPHORUS-32 IN VARYING AMOUNTS OF TRITIUM;  
RATIOS FROM PURE P-32 TO 1 : 5.1.**



**FIGURE 36: PHOSPHORUS-32 IN VARYING AMOUNTS OF TRITIUM;  
RATIOS FROM 1 : 12.5 TO 1 : 31.2.**

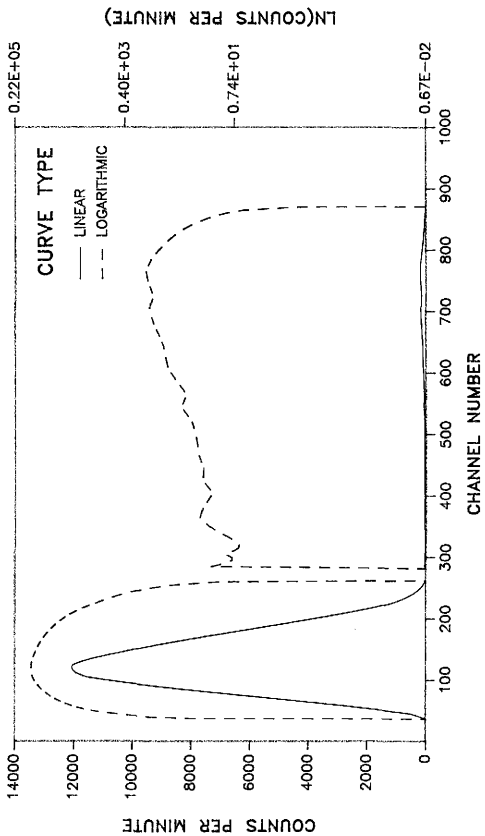
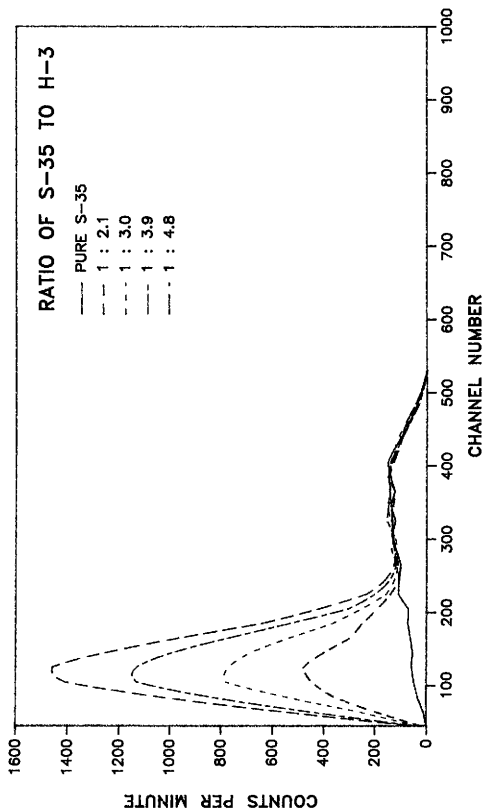
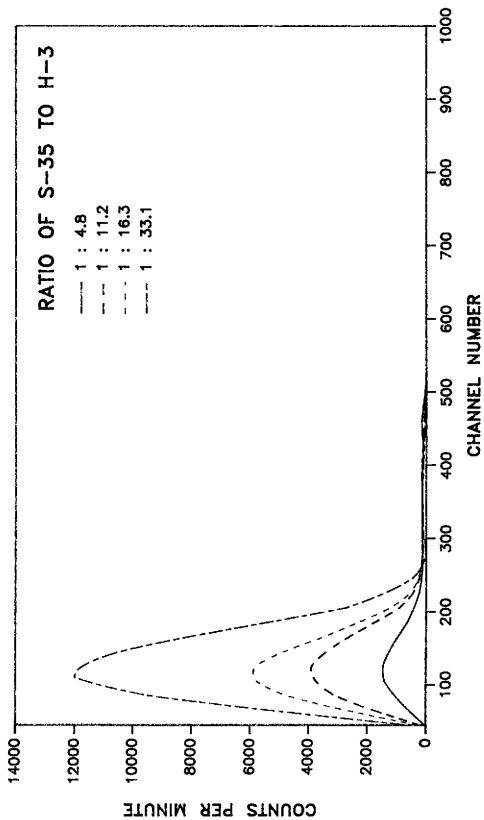


FIGURE 37: COMPARISON OF 1 PHOSPHORUS-32 TO 31.2 TRITIUM ON LINEAR VERSUS LOGARITHMIC SCALES.



**FIGURE 38: SULFUR-35 IN VARYING AMOUNTS OF TRITIUM;  
RATIOS FROM PURE S-35 TO 1 : 4.8.**



**FIGURE 39: SULFUR-35 IN VARYING AMOUNTS OF TRITIUM; RATIOS FROM 1 : 4.8 TO 1 : 33.1.**

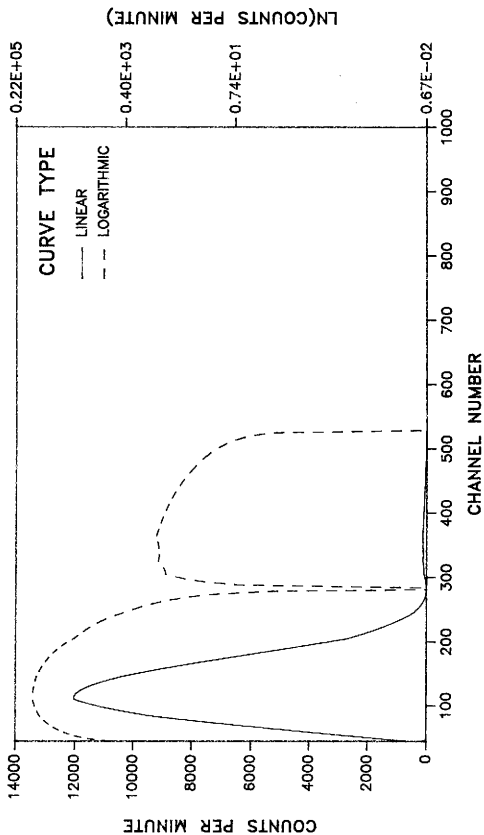
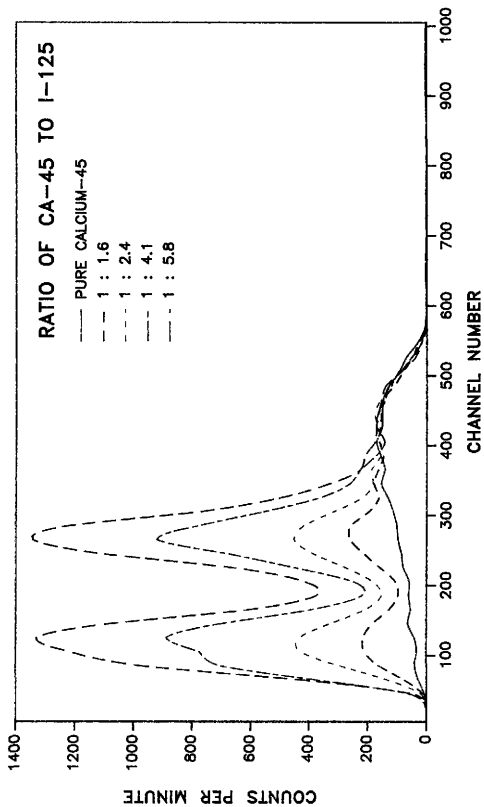


FIGURE 40: COMPARISON OF 1 SULFUR-35 TO 33.1 TRITIUM ON LINEAR VERSUS LOGARITHMIC SCALES.



**FIGURE 41: CALCIUM-45 IN VARYING AMOUNTS OF IODINE-125;  
RATIOS FROM PURE CA-45 TO 1 : 5.8.**

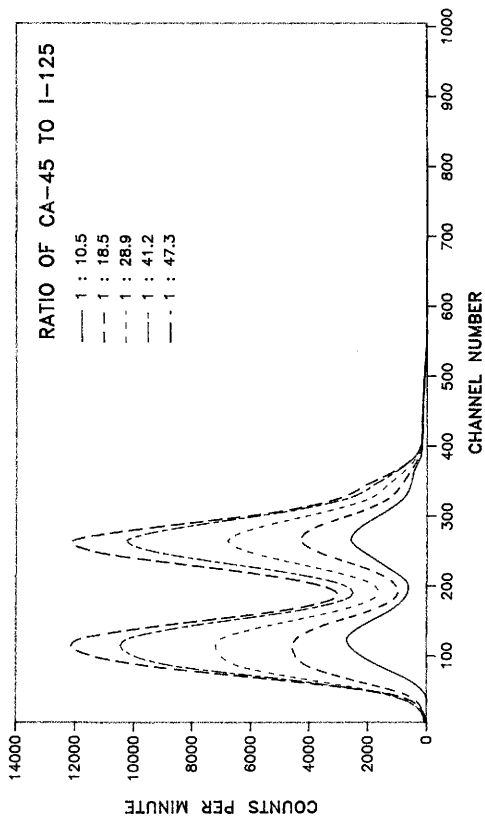


FIGURE 42: CALCIUM-45 IN VARYING AMOUNTS OF IODINE-125; RATIOS FROM 1 : 10.5 TO 1 : 47.3.



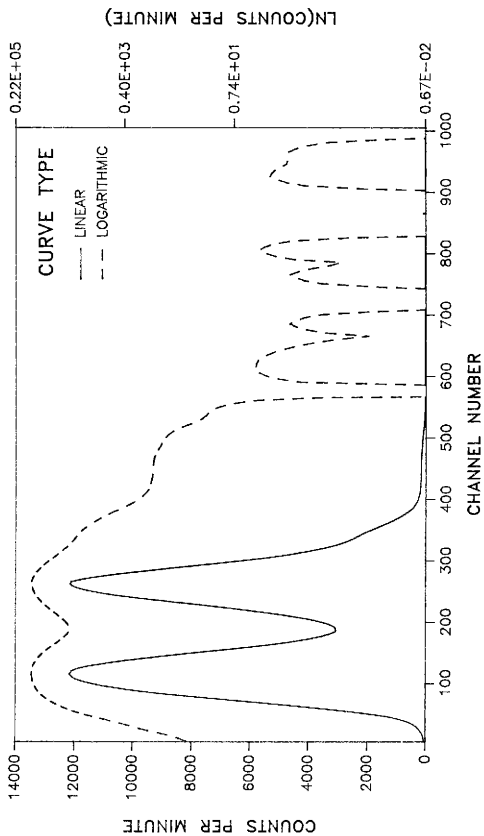
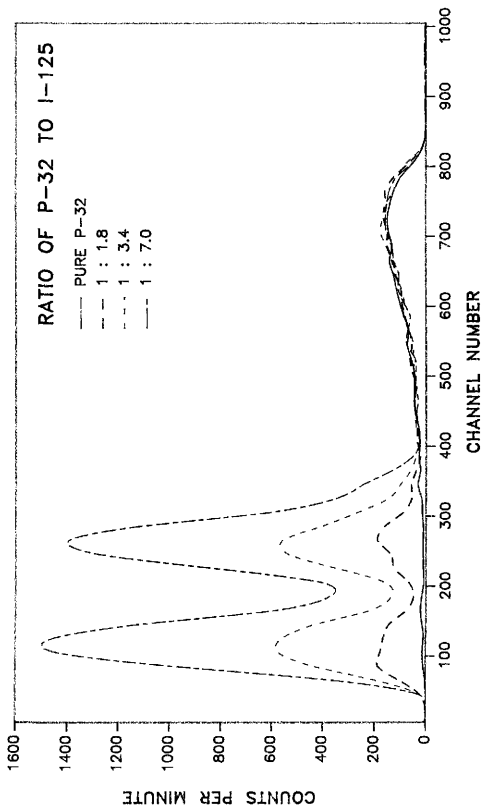


FIGURE 43: COMPARISON OF 1 CALCIUM-45 TO 47.3 IODINE-125 ON LINEAR VERSUS LOGARITHMIC SCALES.



**FIGURE 44: PHOSPHORUS-32 IN VARYING AMOUNTS OF IODINE-125;  
RATIOS FROM PURE P-32 TO 1 : 7.0.**

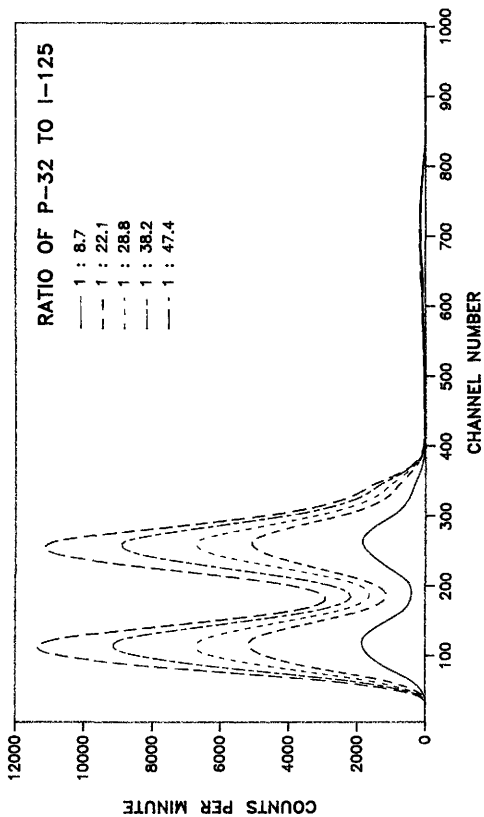


FIGURE 45: PHOSPHORUS-32 IN VARYING AMOUNTS OF IODINE-125; RATIOS FROM 1 : 8.7 TO 1 : 47.4.

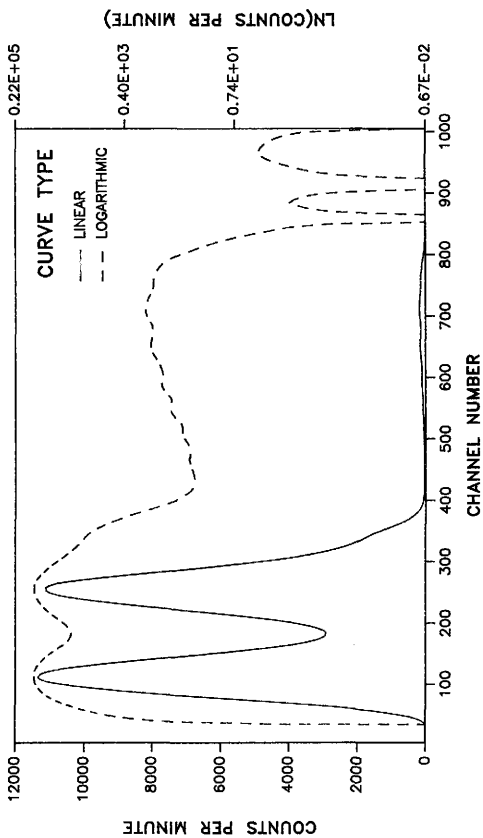


FIGURE 46: COMPARISON OF 1 PHOSPHORUS-32 TO 47.4 IODINE-125 ON LINEAR VERSUS LOGARITHMIC SCALES.

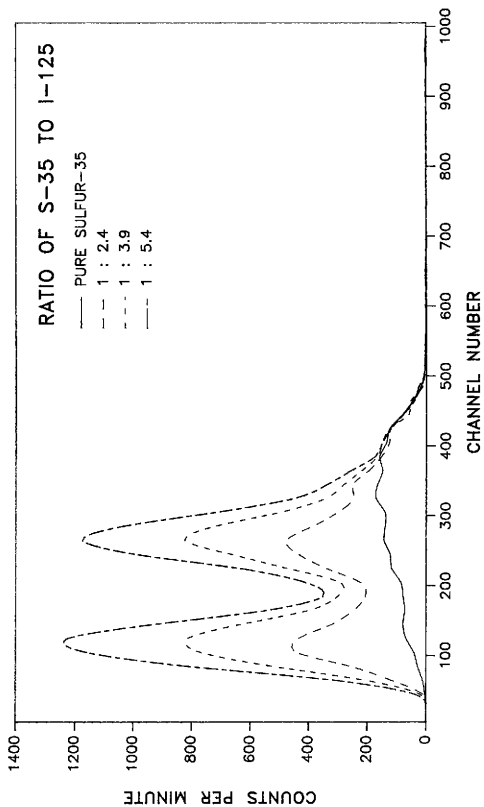


FIGURE 47: SULFUR-35 IN VARYING AMOUNTS OF IODINE-125; RATIOS FROM PURE SULFUR-35 TO 1 : 5.4.

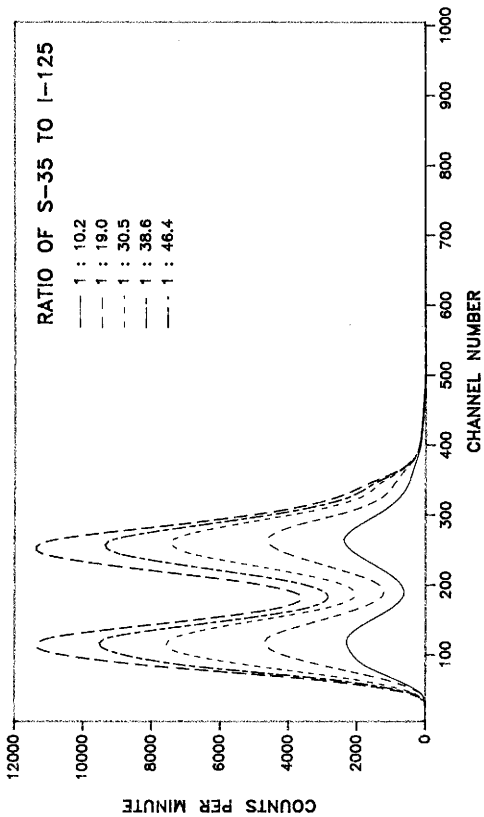


FIGURE 48: SULFUR-35 IN VARYING AMOUNTS OF IODINE-125;  
RATIOS FROM 1 : 10.2 TO 1 : 46.4.

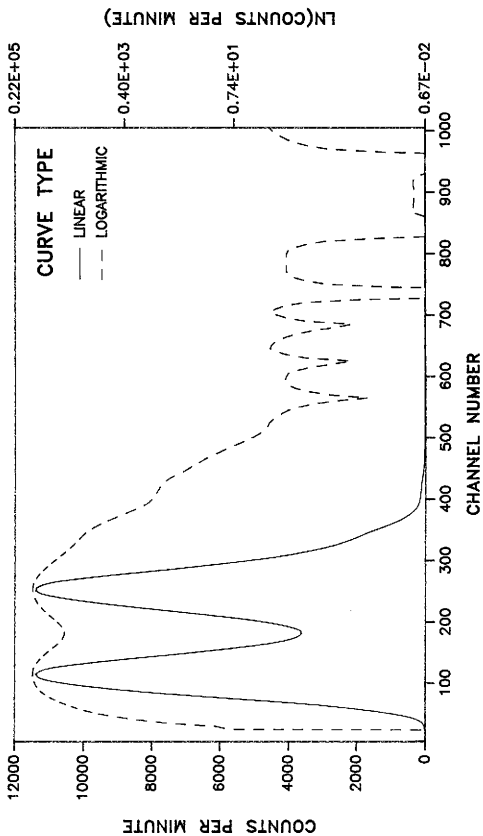


FIGURE 49: COMPARISON OF 1 SULFUR-35 TO 46.4 IODINE-125 ON LINEAR VERSUS LOGARITHMIC SCALES.

## CONCLUSIONS

### CALCULATION OF LLD AND MDA

The derivations, assumptions, and calculations of LLD and MDA are delineated in Appendix D. Note that the values for the counting efficiency are conservative estimates (discussed in Appendix D), and therefore the LLD and MDA values for the research isotopes shown in Table 5 are conservative values also. Furthermore, the LLD and MDA calculations for this research only considered the total cpm for the isotope and background over the complete channel range (5 to 1024) of the detector. When these facts are considered it becomes obvious that such calculated values, which consider only the total cpm of a sample, are much greater than the actual LLD and MDA of samples which have well defined peaks, and a limited energy range such as the radionuclides used in this research. Never the less it should be noted that the calculated LLD and MDA values for all of the isotopes considered are several orders of magnitude less than the regulatory limits for disposal without regard to radioactivity.

### SAMPLE SPECTRA

#### Pure Spectra and Background Data

As previously discussed, the pure spectra of all of the research isotopes are easily recognizable by the energy range, number of peaks, and peak placement. Typical one hour and one minute background counts taken over the channel range of 5 to 1024 were  $109.71 \pm 0.62$  and  $114.94 \pm 9.10$  cpm respectively. The increased standard deviation (one minute count) can be attributed to statistical variations, while the slightly larger cpm is likely due to chemiluminescence. Note that the background addition per channel is so low as to have no significant effect on the shape of sample spectra at the activity levels used in this research.



TABLE 5: CALCULATED LLD AND MDA VALUES.

ISOTOPE	MAXIMUM ENERGY (MeV)	COUNTING EFFICIENCY	LLD (pCi)	MDA (pCi)
H-3	0.0186 $\beta$	35 %	1.00	0.45
Ca-45	0.2570 $\beta^-$ 0.0124 $\gamma$	95 %	0.37	0.17
C-14	0.1560 $\beta^-$	95 %	0.37	0.17
I-125	0.0355 $\gamma$ 0.1770 $E^*$	50 %	0.41	0.31
P-32	1.7100 $\beta^-$	95 %	0.37	0.17
S-35	0.1675 $\beta^-$	95 %	0.37	0.17

#### Reference Spectra

The fastest and most accurate method of isotope identification is simple visual inspection followed by comparison to the reference data generated in this research. Once the closest match to a reference curve is thus determined, the ratio of isotopes in the unknown sample may be considered to be approximately equivalent to that of the reference curve. Table 6 delineates the maximum ratio of a sample isotope mixture that can be easily determined as to isotope content and activity by the methods set forth above.

#### Procedure for Unknown Sample Determinations

The reference data generated allow for a quick and simple screening process for regulatory compliance in waste disposal. If the spectra of an unknown sample are too complex to easily match the reference curves, more conventional methods of determination are indicated. The first and fastest screening process that should be considered in any

TABLE 6: MAXIMUM DETERMINATION LEVELS FOR ISOTOPIC COMBINATIONS.

ISOTOPE	MAX. RATIO FOR EASY IDENTIFICATION OF BOTH ISOTOPES IN A MIXTURE		
	H-3 <sup>1</sup>	C-14 <sup>2</sup>	I-125 <sup>3</sup>
I-125	1 : 50	1 : 27	—
Ca-45	1 : 50	1 : 50	1 : 50
P-32	1 : 50	1 : 50	1 : 50
S-35	1 : 50	1 : 4	1 : 50

<sup>1</sup> Ratio refers to combination of 1 part isotope in left column, to X parts tritium.

<sup>2</sup> Ratio refers to combination of 1 part isotope in left column, to X parts C-14.

<sup>3</sup> Ratio refers to combination of 1 part isotope in left column, to X parts I-125.

sample is whether there is any activity (greater than normal background levels) above channels 525 to 550. Samples with no activity above channel 525 need further inspection, whereas any sample with activity above approximately channel 525 to 550 obviously contain some isotope other than <sup>14</sup>C, <sup>125</sup>I, or <sup>3</sup>H and therefore cannot be considered for disposal without regard to radioactivity.

To determine the isotopes in an unknown sample, the following procedure should be followed.

- (1) Take one minute count of sample on the spectral, using channels 5 through 1024.
- (2) Compare sample X spectrum to reference spectra of pure isotopes (Figure 12) and determine which curve the unknown is most similar to, by peak placement, and/or by spectral energy range.
- (3) Turn to reference spectra for that isotope, and find closest match.
- (4) Data can be uploaded to the VAX and graphed on 'Picture Plus' if an overlay of unknown on reference spectra, or natural log plots are desired.
- (5) Determine ratio of reference curve that is most similar to the unknown, and use as ratio of the unknown sample.
- (6) From curve ratio and total cpm of unknown sample, determine cpm of individual

- isotopes in unknown sample.
- (7) Rough calculation of actual dpm of unknown sample isotopes can be made using estimated efficiency values for the appropriate isotope.

It should be noted that if a suitable match cannot be made, the sample must be assumed to have greater than two isotopes in the mixture, or that a significant amount of quenching is present. Should either be the case, the sample cannot be reliably analysed by the method above.

For example, call the unknown sample, "sample X". Say that the one minute count on the Spectral yielded a spectrum which most closely matched the curve for carbon-14, with 100,000 counts per minute, and had no counts above background from channel 550 to 1024. Comparison of the sample X spectrum would then be made to Figures 15 through 19, and Figures 26 through 28. If, for example, the sample X spectrum most closely matched the 1 : 8.5 ratio curve on Figure 16, it would be assumed that sample X was also approximately 1 part iodine-125 in 8.5 parts carbon-14. Thus it is obvious that sample X has approximately 10,526 cpm of iodine-125 activity, and 89,474 cpm of carbon-14 activity. Then using 50% and 95% values for counting efficiencies of iodine-125 and carbon-14 respectively, one can assume that the unknown sample X has approximately 9.48 nCi of iodine-125, and 0.04  $\mu$ Ci carbon-14. Lastly, multiplying by 10 to account for the total sample size, 0.095  $\mu$ Ci and 0.40  $\mu$ Ci of iodine-125 and carbon-14 respectively, can be assumed to be the isotopes, and activities composing sample X. Thus, sample X could be dispatched of as non-radioactive since the regulatory requirements of less than 0.05 mCi activity of iodine-124, carbon-14, or tritium have been met with proper documentation.

## RECOMMENDATIONS FOR FUTURE RESEARCH

Although compliance with the new waste disposal regulations can be fully met by applying the results of this investigation, several areas need to be expanded. Stock samples used in this study were specifically obtained and checked to be certain that there was an insignificant amount of chemical, water, or color quenching. Actual waste will likely have some degree of quench present. To deal with such samples, a quench curve for each isotope needs to be determined. These quench curves can then be transferred into the 'Multicapture' program. Unknown nuclides present in a sample can be identified by comparison to the reference spectra generated in this research, and as earlier described, the actual activity of each nuclide in the sample calculated. Once this is accomplished the user can have the Spectral automatically determine the counting efficiency for each nuclide using either the single label or dual label function as is appropriate. From these data the user should be able to obtain a more accurate activity value for each sample than is otherwise possible, and then correct for any quenching in the unknown sample. This will also make precise calculations of LLD's and MDA's possible. Entering such data into a computer spread sheet data base (e.g.; LOTUS 1-2-3, or some similar program) would allow for much easier data manipulation, and plot comparisons.

The number of nuclides that can be present in a single sample and still be detected is another area that should be investigated. The research in this thesis could be further expanded to include other isotopes, and combinations of more than two nuclides at a time.

Pattern recognition programs could be extremely useful in spectra analysis of this sort, and further reduce the actual man-hours needed for an accurate determination of the isotopes present, and their activities. Research into the various pattern recognition programs in existence and the modification necessary to fit such codes to this research, or development of a custom code for this type of analysis could be very valuable and cost effective.

A final area that presents itself for study is the possible methods that might be relatively easily and effectively used to chemically or physically separate one or more nuclides from a sample that is too complex to be analysed by spectral data alone, used in conjunction with the techniques in this study.

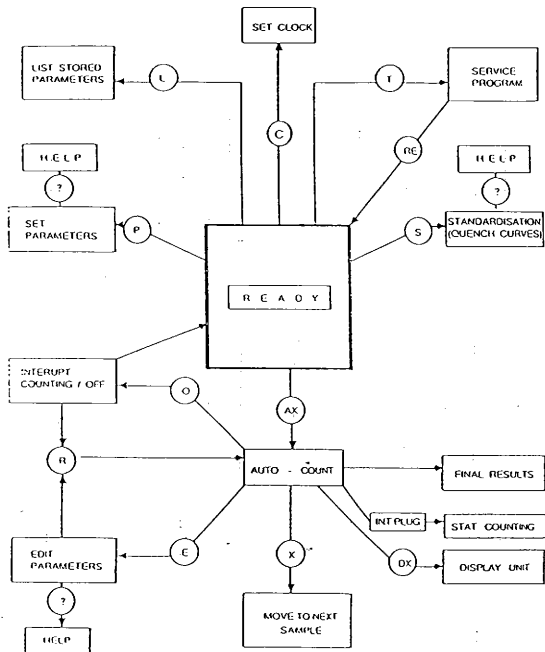
## REFERENCES

- Bi53 Birks J. B., 1953, *Scintillation Counters* (London: Pergamon Press LTD).
- Ce83 Cember H., 1983, *Introduction to Health Physics* (New York: Pergamon Press) 247.
- Co77 Cooper T. G., 1977, *The Tools of Biochemistry* (New York: John Wiley & Sons, Inc.).
- Ed79 Ediss C., Aug. 1979, "A Multichannel Analyzer Interface for a Beckman 9000 Liquid Scintillation Counter," *Liquid Scintillation Counting, Recent Applications and Developments* (New York: Academic Press, Inc.) **1**, 281-289.
- Fo59 Forster T., *Discussions of the Faraday Society* (London: Faraday Society) **27**, 7.
- Ge77 General Electric, 1977, *Chart of the Nuclides*, 12<sup>th</sup> ed. (San Jose, California: General Electric).
- Ha72 Hartley J. H., 1972, "HASL-300 Procedures Manual and Supplements 1-4," *Health and Safety Laboratory* (New York: U.S. Atomic Energy Commission).
- Ho74 Horrocks D. L., 1974, *Applications of Liquid Scintillation Counting* (New York: Academic Press).
- Ka47 Kallmann H., 1947, *Natur und Technik*, July (Germany: Natur und Technik).
- LKB87a LKB-Wallac Company, 1987, "RackBeta 'Spectral' Liquid Scintillation Counter," *1219 Technical Description* (Gaithersburg, Maryland: LKB-Wallac Company) 2-13.
- LKB87b LKB-Wallac Company, 1987, "Added Power With PC," *LKB Diagnostics Informational Packet* (Gaithersburg, Maryland: LKB Diagnostics, Inc.).

- LKB87c LKB-Wallac Company, 1987, *LKB Instrument Manual*, Sect. 4 (Gaithersburg, Maryland: LKB Diagnostics, Inc.) 24.
- Mc87 McLain M. E., Grimes M. J. and Lee P. J., Sept./Oct. 1987, "Evaluation of Dead Time and Gain Shift Correction for a Liquid Scintillation Spectrometer," *Radiation Protection Management* (Kentwood, Michigan; The Techrite Company) **4**, Num. 5, 51-54.
- No79 Noakes J.E. and Spaulding J.D., Aug. 1979, "Pulse Shape Liquid Scintillation Counting For Beta, Gamma or Beta-Gamma Counting," *Liquid Scintillation Counting, Recent Applications and Developments* (New York: Academic Press, Inc.) **1**, 105-117.
- NRC85 Nuclear Regulatory Commission, 1985, *Title 10; Code of Federal Regulations* (Bethesda, Maryland: U. S. Nuclear Regulatory Commission).
- Ot80 Ott C. G., 1980, "Some History of Liquid Scintillation Developed at Los Alamos," *Liquid Scintillation Counting, Recent Applications and Developments* (New York: Academic Press, Inc.) **1**, 105-117.
- S080 Sorenson J. A. and Phelps M. E., 1980, *Physics in Nuclear Medicine* (New York: Harcourt Brace Jovanovich).
- TDH86 Texas Department of Health, Bureau of Radiation Control, April 1986, "21.307 Disposal of Specific Waste," *Texas Regulations for Control of Radiation* (Austin, Texas: Texas Department of Health) **21**, 19.
- Vo63 Voltz G. and Coche, A., 1963, *C.R. Academy of Science* (Paris: The Academy of Science) **1473**, 257.
- Zi80 Zimmer W. H., 1980, *EG&G ORTEC Systems Application Studies*, PSD No. 14 (Tennessee: EG&G ORTEC)

## APPENDIX A

## SPECTROMETER OPERATIONAL FLOW CHART





## APPENDIX B

## PROGRAMS AND COMMAND FILES

## zer0

```

*****
*          This program converts any 0.00 value in a paired dataset to 0.01,      *
*          thus allowing a logarithmic axis in "picsure plus" to be used.      *
*****

CHARACTER * 40 F11, F12
20  WRITE(*,*) 'What file would you like to convert? '
    WRITE(*,*) ', ' (type E or exit to quit)'
    READ(*,25)f11
25  FORMAT(A)
    IF (F11 .EQ. 'E' .OR. F11 .EQ. 'e') THEN
        GO TO 666
    ELSE
        WRITE(*,*)
        OPEN(UNIT=5, FILE=F11, STATUS='UNKNOWN')
        OPEN(UNIT=11, FILE=F11, STATUS='NEW')
10  READ(5,*,end=100)X,Y
        IF(Y .EQ. 0.0) Y = 0.01
        WRITE(11,*)X,Y
        GO TO 10
100 CONTINUE
        WRITE(*,*) 'WE showed that file a thing or three!!!'
        WRITE(*,*)
        WRITE(*,*)
        GO TO 20
    END IF
666 WRITE (*,45)
45  FORMAT (16X,'LATER, 'GATER!')
    END

```

## CONVERT

```
*****
*           This program transforms data uploaded improperly so that carriage *
*           returns and line feed symbols are correct in the data in the VAX file. *
*****
```

```

character*1 line(128),outln(80)
integer posin,posout

c
  posout = 1
  open (unit=50,file='input_file',status='old',recl=128,
  1    recordtype='fixed')
  open (unit=51,file='output_file',status='new',
  1    recordtype='variable',carriagecontrol='list')
  do 5 i=1,80
  5    outln(i) = ''
c
  10    read(50,11,end=999) (line(i), i=1,128)
  11      format (128a1)
        posin = 1
  200    if (ichar(line(posin)).eq.0) then
        posin = posin + 1
        goto 500
    end if
        if (ichar(line(posin)).eq.13) goto 300
        if (ichar(line(posin)).eq.10) goto 400
        outln(posout) = line(posin)
        posin = posin + 1
        posout = posout + 1
    goto 500
  300    posin = posin + 1
        if (posin.gt.128) goto 10
  400    posin = posin + 1
        write (51,13) (outln(j), j=1,80)
  13      format (80a1)
        do 401 j=1,80
  401      outln(j) = ''
        posout = 1
  500    if (posin.gt.128) goto 10
        goto 200
  999    continue
        stop
        end

```

## PARAMETERS

```
*****
*           This command file is used for linear X axis graphs           *
*           on 'Picture Plus' graphs.                                     *
*****
```

```
/*
/* CHART DEFINITION COMMANDS
/*
LINE CHART
PICTURE WINDOW 23.0000 15.5000 CM
DISABLE PICTURE BACKGROUND
CHART WINDOW 1.000 99.000 1.000 99.000
DISABLE CHART BACKGROUND
DATA WINDOW 13.000 95.000 27.000 97.000
LEGEND POSITION AUTO
/*
/* TEXT DEFINITION COMMANDS
/*
NOTE 1
FIGURE X: XYZ'
TEXT POSITION 50.00 7.28
CURRENT AXIS BOTTOM
AXIS LABEL
'CHANNEL NUMBER'
CURRENT TEXTITEM BOTTOM TICK LABELS
/*
CURRENT AXIS LEFT
AXIS LABEL
'COUNTS PER MINUTE'
AXIS TYPE LINEAR
/*
DISABLE TOP TICK NUMBERS
/*
DISABLE RIGHT TICK NUMBERS
CURRENT TEXTITEM LEGEND ENTRIES
CURRENT TEXTITEM BAR NUMBERS
```

## PARALOG

```
*****
*           This command file is used for natural logarithmic X axis graphs           *
*           on 'Picture Plus' graphs.                                               *
*****
```

```
/*
/* CHART DEFINITION COMMANDS
/*
LINE CHART
PICTURE WINDOW 23.0000 15.5000 CM
DISABLE PICTURE BACKGROUND
CHART WINDOW 1.000 99.000 1.000 99.000
DISABLE CHART BACKGROUND
DATA WINDOW 13.000 85.000 27.000 97.000
LEGEND POSITION 50.000 7.280
```

```
/*
/* TEXT DEFINITION COMMANDS
/*
NOTE 1
'FIGURE X: XYZ'
TEXT POSITION 50.00 7.28
CURRENT AXIS BOTTOM
AXIS LABEL
'CHANNEL NUMBER'
CURRENT TEXTITEM BOTTOM TICK LABELS
```

```
/*
CURRENT AXIS LEFT
AXIS LABEL
'COUNTS PER MINUTE'
AXIS TYPE LINEAR
CURRENT TEXTITEM LEFT TICK LABELS
```

```
/*
CURRENT AXIS RIGHT
AXIS LABEL
'LN(COUNTS PER MINUTE)'
AXIS TYPE LOGN
TICK NUMBERS (E8.2)
```

```
/*
DISABLE TOP TICK NUMBERS
/*
CURRENT TEXTITEM LEGEND ENTRIES
CURRENT TEXTITEM BAR NUMBERS
```

## APPENDIX C

### CALCULATION OF LLD's AND MDA's

A calculation of the Minimum Detectable Activity (MDA) for each radionuclide is necessary to give an accurate indication of the maximum nuclide activity that could remain undetected (Zi80). Calculation of MDA's incorporates a user determined sensitivity level, and are reported as 'less than' values in terms pCi within a  $1\sigma$  precision level. In order to calculate the MDA, one must first determine the lower limit of detection (LLD) for the Spectral. The LLD as defined by Harley (Ha72) is:

The smallest amount of sample activity, using a given measurement process (i.e., chemical procedure and detector) that will yield a net count for which there is confidence at a predetermined level that activity is present.

The definition of LLD is shown mathematically in equation 11.

$$LLD \approx (K_{\alpha} + K_{\beta}) S_o \gamma \quad (11)$$

Where  $K_{\alpha}$  is the the preselected risk of a type one error,  $K_{\beta}$  the preselected risk of a type two error (i.e. concluding that activity is not present when in fact it is present.),  $S_o$  is the standard error for the net counting rate of the sample, and  $\gamma$  is the conversion factor from count rate to activity for a given isotope. Letting  $K_{\alpha} = K_{\beta} = 5\%$ , and setting the counting time for background equal to the counting time for the sample (as was the case throughout this research), the LLD equation may then be written as shown in equation 12. Where  $S_b$  is the typical background count rate (for this research,  $S_b$  was the the background from

channel 5 to 1024).

$$\text{LLD} \approx 2K\sqrt{2S_b}\gamma \quad (12)$$

Thus, setting the risk of type one and type two errors to be 5%, it is obvious that equation 12 may now be written as is equation 13.

$$\text{LLD} = 4.66\sqrt{S_b}\gamma \quad (13)$$

Now  $\gamma$  may be found using equation 14.

$$\gamma = \frac{1}{\text{RVEDA}\sqrt{t}} \quad (14)$$

Where R is the chemical yield or recovery for all steps within the procedure (set to 1 in this instance since there is no recovery or yield to consider.), V is the volume of the sample (again set to 1 since sample volume does not have effect in LSC.), E equals the counting efficiency of the detector for the nuclide of interest, D is the radioactive decay fraction, A the unit conversion factor (i.e., 2.22 pCi/dpm), and t equals the counting interval. The radioactive decay factor in this case may also be set to one assuming that all samples are counted prior to a significant time lapse for decay. Thus the equation has evolved to:

$$\text{LLD} = 4.66\sqrt{S_b}\frac{1}{E2.22\sqrt{t}} \quad (15)$$

Now  $t$  may be set to 60 seconds, and  $S_b$  to 6000 cps (100cpm) or the average background counts in one minute on the Spectral.

At this point several assumptions must be made as to the counting efficiency of the Spectral for the different isotopes used in this research. As traceable standards were not available, the Spectral counting efficiencies for the isotopes studied were estimated. Operating specifications for the Spectral quote a counting efficiency for  $^3\text{H}$  and  $^{14}\text{C}$  as 70.1% and 96.9%, respectively. Data for other isotopes was not included. It must be noted that these efficiencies were under ideal conditions, with non-aqueous samples, and absolutely no quenching or other interference. Real efficiency, under typical laboratory conditions, and with normal samples can be expected to be lower. The Yankee Atomic Environmental Laboratory estimates ~30% efficiency for  $^3\text{H}$ , and ~90% for  $^{14}\text{C}$ . For a conservative estimate of the LLD, the Spectral's efficiency was assumed to be 35% and 95% for  $^3\text{H}$  and  $^{14}\text{C}$  respectively. A further estimation was made for the counting efficiencies of  $^{125}\text{I}$ ,  $^{45}\text{Ca}$ ,  $^{32}\text{P}$ , and  $^{35}\text{S}$  by considering their beta decay energies. Thus, an efficiency of 95% was used for  $^{45}\text{Ca}$ ,  $^{32}\text{P}$ , and  $^{35}\text{S}$ , while the lower energy  $^{125}\text{I}$  was assumed to have an efficiency of 50%.

Using the above values, the LLD was calculated to be 1.00 pCi for  $^3\text{H}$ , 0.41 pCi for  $^{125}\text{I}$ ; and 0.37 pCi for  $^{14}\text{C}$ ,  $^{45}\text{Ca}$ ,  $^{32}\text{P}$ , and  $^{35}\text{S}$ .

Now the MDA for 1 $\sigma$  precision may be calculated using Equation 16.

$$\text{MDA} = \frac{C}{E133.2\sqrt{t}} \left[ \left( 2\sqrt{S_b} + \frac{C}{4} \right) + \frac{C}{2} \right] \quad (16)$$

Where C is defined as 100 divided by the percent sensitivity set by the user (C must be multiplied by 1.96 and 2.58 for 2 $\sigma$  and 3 $\sigma$  output respectively.). Thus if 95% sensitivity is

used for all samples the MDA is found to be  $< 0.45$  pCi for  $^3\text{H}$ ,  $< 0.032$  pCi for  $^{125}\text{I}$ ; and  $< 0.17$  pCi for  $^{14}\text{C}$ ,  $^{45}\text{Ca}$ ,  $^{32}\text{P}$ , and  $^{35}\text{S}$  (See Table 5).



## VITA

Robin Lynn Siskel was born 30 August 1962, in Modesto, California. She is the daughter of Maurice and Valerie Siskel, Jr. She attended high school in Alabama and Texas, graduating in 1979 with honors from Richland High School, Ft. Worth, Texas.

After a year long internship with an Olympic calibre riding instructor, she attended Texas A&M University as a National Merit Scholar, and in August 1985, received a Bachelor of Science degree in Biochemistry. Upon graduation she enrolled in the Graduate College at Texas A&M University to pursue a Master of Science degree in Health Physics. In 1986 she was a summer intern at The Oak Ridge National Laboratory's Dosimetry Applications Research Facility. Throughout graduate school she held a research assistantship position for the Department of Nuclear Engineering, and presented several award winning papers at professional society meetings.

Her permanent address is:

Robin Siskel  
P.O. Box 4585  
College Station, TX  
77844

She can also be reached through the Department of Nuclear Engineering, Room 129 Zachry Engineering Building, Texas A&M University, College Station, TX 77843.